Available online at www.sciencedirect.com

ScienceDirect

journal homepage: www.elsevier.com/locate/he

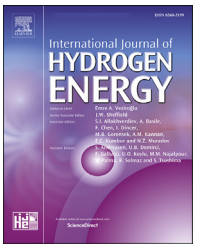

Review Article

Recent progress in lithium-ion battery thermal management for a wide range of temperature and abuse conditions

Z.Y. Jiang [a], H.B. Li [b], Z.G. Qu [b,*], J.F. Zhang [b]

[a] School of Chemical Engineering and Technology, Xi'an Jiaotong University, Xi'an, Shaanxi, 710049, China
[b] MOE Key Laboratory of Thermo-Fluid Science and Engineering, School of Energy and Power Engineering, Xi'an Jiaotong University, Xi'an, Shaanxi, 710049, China

HIGHLIGHTS

- The investigations on the lithium ion battery thermal management is reviewed.
- The air, liquid, PCM and combined cooling methods are discussed.
- The external, alternating current and self-heating methods are analyzed.
- The thermal runaway mechanism and prevention methods are discussed.
- Research challenges and directions for future studies are provided.

ARTICLE INFO

Article history:
Received 6 December 2021
Received in revised form
30 December 2021
Accepted 3 January 2022
Available online xxx

Keywords:
Lithium-ion battery
Thermal management
Heat generation
Cooling method
Heating method
Thermal runaway

ABSTRACT

Lithium-ion batteries are important power sources for electric vehicles and energy storage devices in recent decades. Operating temperature, reliability, safety, and life cycle of batteries are key issues in battery thermal management, and therefore, there is a need for an effective thermal-management system. This review summarises the latest research progress on lithium-ion battery thermal management under high temperature, sub-zero temperature, and abuse conditions. Heat generation mechanisms are characterised under both normal and abuse conditions. Different cooling methods, which include air cooling, liquid cooling, phase change cooling, heat pipe cooling, and their combinations are reviewed and discussed. Thereafter, features of different battery heating methods such as air/liquid heating, alternate current heating, and internal self-heating are discussed. An improvement in battery safety under abuse conditions is discussed from the perspective of battery material modification and thermal management design. The research progress in recent investigations is summarised, and the prospects are proposed.

* *Corresponding author.*
E-mail address: zgqu@mail.xjtu.edu.cn (Z.G. Qu).

https://doi.org/10.1016/j.ijhydene.2022.01.008
0360-3199/

Please cite this article as: Jiang ZY et al., Recent progress in lithium-ion battery thermal management for a wide range of temperature and abuse conditions, International Journal of Hydrogen Energy, https://doi.org/10.1016/j.ijhydene.2022.01.008

Contents

Introduction

The use of fossil fuels in the past few centuries has induced environment issues such as global warming and air pollution. Looking for new energy that can replace fossil energy has become an urgent task. At present, advanced new energy technologies can efficiently convert nuclear, wind and solar energy into electrical energy [1]. Lithium–ion batteries (LIBs) is a dominating electrochemical energy source which is widely used in electric vehicles (EVs) and energy storage. LIBs have maintained rapid growth in sales because of their high energy density and prolonged life cycle compared to other rechargeable battery systems. A comparison of the energy density, cost, and life of LIBs and other battery systems is illustrated in Table 1. The global market for LIBs has rapidly grown because of the increasing demand for EVs in recent years.

In order to provide high energy density, lightweight design and long-life battery power supply, an effective battery management system (BMS) is necessary [7,8]. The battery thermal management system (BTMS) is an important sub-system of BMS. The battery performance and battery life cycle of LIB are highly sensitive to temperature, and high temperatures can significantly accelerate the degradation of LIBs [9]. Therefore, LIBs are recommended to be utilised within the optimum temperature range of 20–45 °C. Efficient battery cooling and heating methods are critical LIB applications.

The battery cooling at high temperature environment is necessary. The high temperature causes the rapid growth of the solid electrolyte interface (SEI) on the surface of the electrode particle [10]. The growth of SEI increases the battery impedance and reduces the battery power, and the lithium consumed by SEI growth causes capacity decline. Moreover, the thermal runaway (TR), a severe safety issue, can occur with insufficient heat dissipation in the battery [11,12]. The TR process comprises the battery temperature increment and the battery material decomposition. Complex reactions including reactions between positive material, negative material, electrolyte and binder can occur inside the battery [13]. TR is generally induced by serious abuse conditions which include mechanical [14–16], electrical [17], and thermal abuse [18]. Collisions, crashes, and penetrations are common mechanical

Table 1 – Comparison of different battery systems.

	Lead acid [2]	Lithium ion [3]	Na–S [4]	Redox flow battery [5,6]
Cycle life	500–5000	1000–20000	4000–5000	20,000
Working temperature (°C)	−40–60	−30–55	300–350	10–40
Energy density (Wh/Kg)	35–55	90–260	130–150	25–40
Energy efficiency (%)	50–75	Around 95	75–90	65–82
Depth of discharge (%)	<70	100	>90	100
Self-discharge rate (%/Mon)	4–50	<2	N/A	3–9

Please cite this article as: Jiang ZY et al., Recent progress in lithium-ion battery thermal management for a wide range of temperature and abuse conditions, International Journal of Hydrogen Energy, https://doi.org/10.1016/j.ijhydene.2022.01.008

Table 2 – Review articles about BTMS in recent years.

Reference	Publish year	Key words	Focus of literature	Remarks
Liu et al. [30]	2017	Li-ion battery, Temperature effect, Battery modelling, Thermal management system, Phase change	Modelling of BTMS and different cooling strategies	Thermal model, electrochemical model, equivalent circuit model and electrochemical/electrical-thermal coupling methods; BTMS using including the air, liquid, boiling, heat pipe and solid-liquid phase change based strategies.
Xia et al. [31]	2017	Electric vehicle, Lithium ion battery, Thermal management system, Temperature distribution, Cooling configuration	Cooling strategies for cell level and module level thermal management	Heat generation, heat transport, and heat dissipation for single cell; battery module based on different cooling methods and cooling configuration.
Deng et al. [32]	2018	Coolants, Cooling strategies, Cooling performance, Power lithium ion battery system	Liquid cooling system with different coolants and cooling strategies	Performance of coolant, classification of liquid cooling system and design of battery pack.
Feng et al. [33]	2018	Lithium ion battery, Electric vehicle, Thermal runaway, Battery safety, Internal short circuit	Mechanism of thermal runaway and its propagation	Clarify the reaction kinetics using energy release diagram; propose three-level protection concept of reducing TR hazard.
Chen et al. [34]	2019	Li-ion battery, Thermal management system, Cooling performance, Phase change material	Phase change material based thermal management method	PCM-based passive BTMS; enhancement of PCM performance; hybrid BTMS.
Peng et al. [35]	2019	battery pack, cold temperatures, estimation, heating methods, lithium-ion batteries	Thermal management at low temperature	Comprehensive study on the aging mechanisms of lithium- ion batteries at cold temperatures; estimation methods of SOH; battery heating methods.
Wu et al. [36]	2019	Electric vehicle, Temperature effect, Battery thermal management, Liquid,	Liquid based thermal management system	Thermal performance at low temperature, high temperature and differential temperature; systematic review of direct and indirect liquid based BTMS; phase change cooling and heat pipe.
Akinlabi et al. [37]	2020	Air cooling, Battery thermal management system, Electric vehicle, Lithium-ion, Optimisation	Air-cooled thermal management system	Air-cooled BTMS techniques (passive and active) and design parameter optimisation methods for improving various BTMS design objectives.
Karthik et al. [38]	2020	Air cooling-based battery thermal management systems, Electric vehicles, Liquid cooling based battery thermal management systems, Lithium-ion battery pack, Phase change cooling based battery thermal management systems, Temperature non-uniformity, temperature rise	Thermal runaway failure prevention	Thermal management issues under extreme temperature conditions.

(*continued on next page*)

Table 2 – (continued)

Reference	Publish year	Key words	Focus of literature	Remarks
Duan et al. [39]	2020	Electric vehicles, Lithium-ion battery, Safety, Batteries design, Real-time monitoring	Safety of LIB material and battery monitoring	Safety features of LIBs and the failure mechanisms of cathodes, anodes, separators and electrolyte; solutions for designing safer components
Tete et al. [40]	2021	Battery thermal management system Electric vehicles; E– vehicles; Battery cooling Lithium-ion; Air cooling; Liquid cooling	Air cooling; liquid cooling; PCM cooling	Practical BTM techniques for EV applications

abuse conditions which can cause a short circuit to the battery. The external short circuit [19,20], over-charge [21], and over-discharge [22]are electrical abuse conditions which induces the penetration or breakdown of the separator and causes the corresponding internal short circuit in the battery. The internal short circuit caused by mechanical and electrical abuse induces instantaneous electric energy release and causes a tremendous joule heating. As a result, the battery is heated to extreme temperatures with this released joule heat and the TR is initiated.

The temperature control of LIB at low temperatures is necessary for realistic applications. LIBs suffer severe performance degradation at low temperatures, which is induced by the slowdown of species transfer and chemical reactions. The electrolyte conductivity [23] and electrode ion diffusivity [24] both decrease significantly when battery temperature dropped from room temperature to sub-zero temperature. The decrease in electrolyte conductivity and lithium diffusivity increased the battery resistance significantly. Zhang et al. [25] reported that internal resistance increases 10 times as the cell temperature is decreased by 40 °C. The available energy, power, and capacity were affected by the decreased specie transfer process of a battery. As a result, only 12% battery capacity could be achieved at −40 °C compared with that at room temperature [26]. The reduced transport kinetics caused significant polarization at electrode particle surface. The lithium deposition process on the anode surface are accelerated during battery charging [27], which reduces the battery capacity. Moreover, as indicated by research of Feng et al. [28], a significant exothermic reaction peak occurs at a lower temperature and consumes electrolyte. Further investigation of Li et al. [29] reveals that the reactions between plated Li and electrolytes account for the early eruptions at 110 °C during adiabatic TRs. In addition to the exothermic effect of lithium plating, the deposited lithium metal formed dendrite, which may cause an internal short circuit and TR in the battery. Therefore, efficient heating strategies are required to warm the battery to achieve an adequate start-up temperature.

A robust LIB thermal management system is critical for LIB applications. A BTMS should be able to solve issues such as battery cooling, battery warming, and prevention of thermal runaway propagation. We surveyed the review papers [30–40] in the recent three years on LIB thermal management to draw a clear outline of the investigations on LIB thermal management. Detailed information for each review paper is provided in Table 2. The LIB thermal management has been widely investigated in recent years. Relevant studies include LIB modelling, cooling strategies, battery performance at low temperatures, battery heating strategies, battery thermal runaway, and prevention methods. Liquid cooling and phase change material (PCM) cooling are the commonly used methods for cooling strategies. Most recent review papers only involve one or two aspects of battery thermal management, and therefore, it is essential to provide a comprehensive discussion of battery thermal management under a wide temperature range and abuse conditions.

In this review, an overview of recent research on LIB thermal management is provided. The rest of this review is organised as follows: The heat generation mechanism is discussed and the heat source calculation under normal and

Please cite this article as: Jiang ZY et al., Recent progress in lithium-ion battery thermal management for a wide range of temperature and abuse conditions, International Journal of Hydrogen Energy, https://doi.org/10.1016/j.ijhydene.2022.01.008

abuse conditions is determined in Section Energy balance in lithium-ion battery. Then, the battery cooling and heating strategies are reviewed in section Battery cooling method at high operating temperature and Battery heating at sub-zero temperature. The heat generation during TR, mitigation of TR and the prevention of TR propagation are discussed in Section Prevention strategies for thermal runaway. Finally, we present the conclusion and future perspective on the development of LIB thermal management in Section Summary and Prospect.

Energy balance in lithium-ion battery

Heat generation mechanism

Battery thermal management should begin with the understanding of energy balance and heat transfer in the battery. The following energy balance equation is the basis for building a thermal model of a battery under working conditions:

$$\rho_{cell} c_{p,cell} \frac{\partial T_{cell}}{\partial t} = \nabla \cdot (k_{cell} \nabla T_{cell}) + \dot{Q} + \dot{Q}_{ext} \quad (1)$$

As shown in Eq. (1), the term on the left-hand side is the temporal change in the battery temperature, and the first term on the right-hand side represents the spatial change in the battery temperature. $Q(\bullet)$ represents the heat generation inside the battery, and $Q(\bullet)_{ext}$ represents the heat exchange between the battery and exterior cooling/heating structure. The battery heat generation rate, heat dissipation, and the specific heat capacity of the battery need to be determined to identify the temperature change in the battery. Heat generation is inevitable during LIB applications. The internal heat originates in batteries majorly from the following three sources: i) polarization losses (activation, concentration, and ohmic polarizations); ii) entropy change from battery electrochemical reaction and side reaction; and iii) heat from the mixing process during battery relaxation [41]. A theoretical analysis of heat generation during the electrochemical process is illustrated as [42,43]:

$$\dot{Q} = \dot{Q}_{jou} + \dot{Q}_{re} + \dot{Q}_{sr} + \dot{Q}_{mix} = I(U - V) - I\left(T\frac{\partial U}{\partial T}\right) - \sum_i \Delta H_i^{avg} r_i - \int \sum_j \left(\overline{H}_j - \overline{H}_j^{avg}\right) \frac{\partial c_j}{\partial t} dv \quad (2)$$

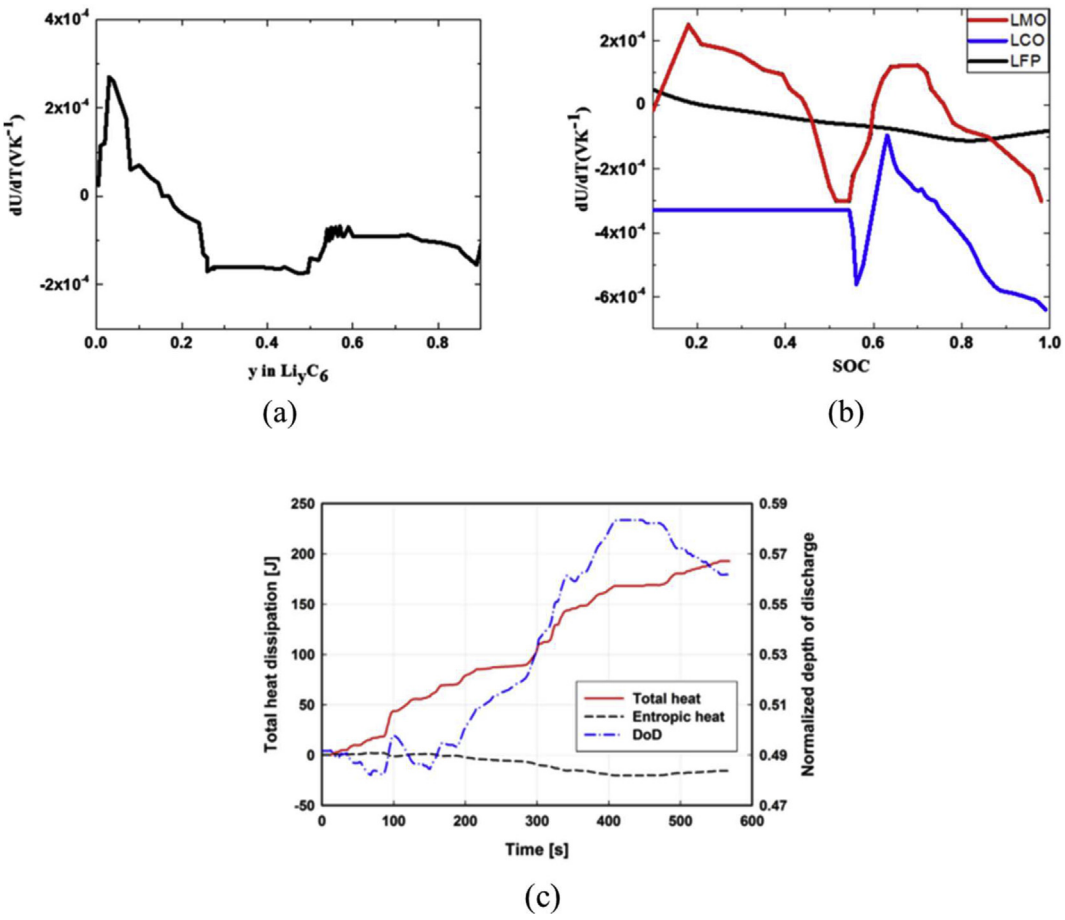

Fig. 1 – Entropy heat coefficient and heat generation calculation: (a) entropy heat coefficient of graphite anode [51]; (b) entropy heat coefficient of different cathode material [51]; (c) heat generation rate calculated using the P2D model [52].

Please cite this article as: Jiang ZY et al., Recent progress in lithium-ion battery thermal management for a wide range of temperature and abuse conditions, International Journal of Hydrogen Energy, https://doi.org/10.1016/j.ijhydene.2022.01.008

The first term $Q(\bullet)_{jou}$ on the right-hand side of the heat source is the irreversible Joule heat, the second term $Q(\bullet)_{re}$ is the heat of the reaction entropy change, the third term $Q(\bullet)_{sr}$ accounts for the heat of the side reaction, and the last term $Q(\bullet)_{mix}$ represents the heat from the mixing process. The heat of the side reaction and mixing process can be ignored for most small format batteries under constant current testing and without serious degradation. Therefore, heat from the following simplified form of the heat generation equation is cited in most studies focused on BTM issues [44].

$$\dot{Q} = \dot{Q}_{jou} + \dot{Q}_{re} = I(U - V) - I\left(T\frac{\partial U}{\partial T}\right) \quad (3)$$

Heat generation in the simplified form comprises irreversible Joule heat and reversible entropic heat. However, in realistic application, the heat generation characteristic changes with the aging of the battery, which is attributed to the fact that the internal resistance of the battery increases with the battery aging [45,46]. The value of the heat generation rate of a single cell can be obtained by both numerical analysis and experimental testing. For a numerical method, the well-known pseudo two-dimensional (P2D) model is commonly utilised to determine battery heat generation characteristics. This model was established by Newman et al. [47] The value of heat generation is obtained by the P2D model under the given working conditions and battery thermal properties [48]. Irreversible heat generation can be obtained when the polarization of the battery is determined; reversible heat comprises the current and entropy heat coefficients. The entropy heat coefficient (dU/dt) is commonly illustrated as a function of state of charge (SOC) and is mostly obtained by experimental measurements because it changes with battery chemistries [49]. Therefore, the accurate prediction of SOC is important for the determination of battery heat generation [50]. Fig. 1(a and b) shows the typical curves of the entropy heat coefficient of different electrode materials. Advantages of using the numerical simulation to determine heat generation include the irreversible joule heat and reversible heat that can be separated from each other, as indicated in Fig. 1 (c).

Heat generation can be measured experimentally. The most commonly used experimental methods include accelerated-rate calorimetry (ARC) and isothermal heat conduction calorimetry (IHC), as shown in Fig. 2(a and b). The ARC is capable to investigate exothermic chemical reactions by providing a simulated adiabatic condition, and the ARC measures the heat generation rate at an increasing battery temperature. Important kinetic parameters such as the enthalpy of the exothermic process and the reaction onset temperature

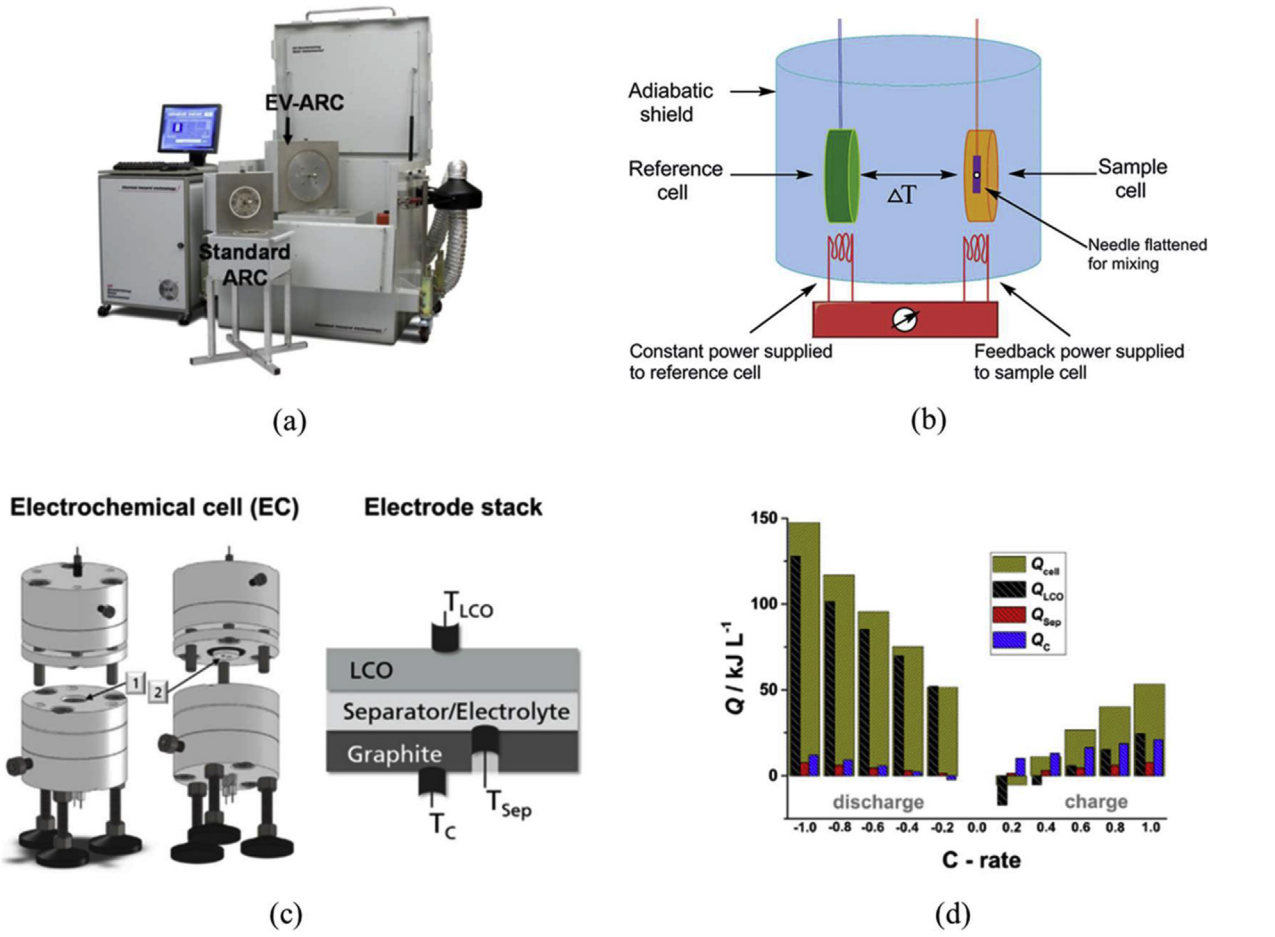

Fig. 2 – Measurement of battery heat generation: (a) ARC testing [11]; (b) IHC testing [58]; (c) custom build testing module for heat generation [59]; (d) heat generation rate in each battery component [59].

Please cite this article as: Jiang ZY et al., Recent progress in lithium-ion battery thermal management for a wide range of temperature and abuse conditions, International Journal of Hydrogen Energy, https://doi.org/10.1016/j.ijhydene.2022.01.008

can be obtained by ARC in addition to the heat generation rate [53,54]. Differently, the heat generation measured by IHC is fixed at a certain temperature [55–58]. The thermal stability of the battery material can be evaluated by IHC. Many studies have been conducted to measure the battery heat generation rate for different LIB types and at different C-rates. Heat generation within the individual components of the battery cell, which include the negative electrode, separator, and positive electrode, distinctly differs because of the different material properties and electrochemical kinetics and thermodynamics. Therefore, the heat generated in each part of the battery must be clarified. Heubner et al. [59] measured the local in-operando temperature of the cell using utilised a self-innovate electrochemical cell, which is shown in Fig. 2(c and d). Further, they compared the measured heat generation rates with those calculated using galvanostatic intermittent titration technique measurements.

Determination of thermal conductivity and specific heat capacity

The most important thermal properties of lithium-ion batteries include their specific heat capacity and thermal conductivity. Most lithium-ion batteries comprise a layered structure that includes a cathode, anode, separator, and two current collector layers. The basic unit of the battery comprises an anode layer, one cathode layer, one separator, and two current collectors. The thickness of each layer is less than 100 μm. The

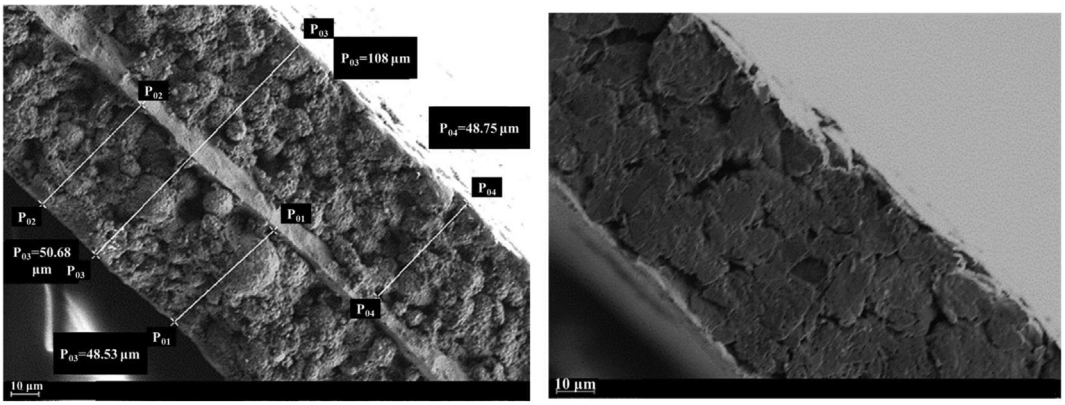

Fig. 3 – SEM figures of the cathode and anode layers.

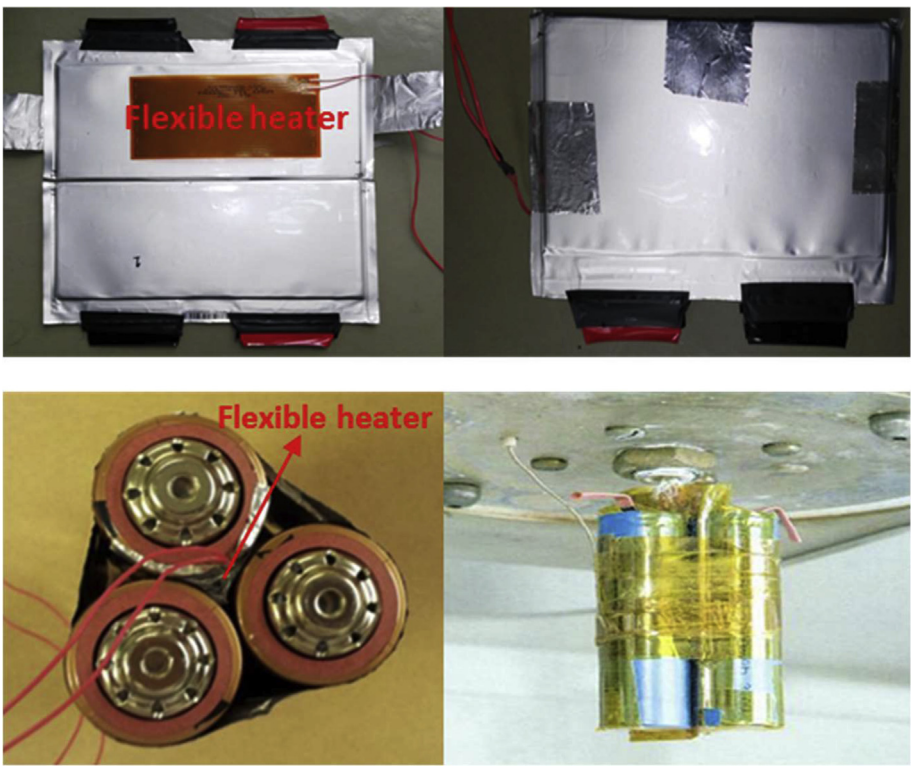

Fig. 4 – Measurement of the battery specific heat capacity in ARC.

Please cite this article as: Jiang ZY et al., Recent progress in lithium-ion battery thermal management for a wide range of temperature and abuse conditions, International Journal of Hydrogen Energy, https://doi.org/10.1016/j.ijhydene.2022.01.008

Table 3 – Summary of recent development of air-cooled BTMS.

No.	Cooling system	Heat transfer coolant	Battery type	Type of study	Battery load	T_{max} (°C)	ΔT_{max} (°C)	Variables/Remarks	Year	References
1	Forced Air-cooling	Air	N × M prismatic battery cells	Numerical	5C	47.3	10.3	Initial cell spacing distribution and step length of the cell spacing adjustments,	2018	Chen et al. [67]
2	Forced Air-cooling	Air	N × M prismatic battery cells	Numerical	5C	43.4	5.6	Angles of the plenums and the widths of the inlet and the outlet	2018	Chen et al. [68]
3	Forced Air-cooling	Air	Panasonic NCR18650 lithium-ion battery	Numerical	2C	–	2.58	Variation of inter-cell spacing on cooling efficiency, air flow velocity and discharge rate	2021	Kirad et al. [69]
4	Forced Air-cooling	Air	32 cylindrical lithium-ion batteries	Experiment	1C/2C	–	–	Aligned, staggered, and cross battery packs arrangement	2019	Fan et al. [70]
5	Forced Air-cooling	Air	Commercial 18,650 lithium ion battery	Numerical	0.5C	29.45	–	Cooling channel size and air supply strategy	2018	Lu et al. [71]
6	Forced Air-cooling	Air	Commercial Sanyo 18,650 lithium-ion battery	Numerical	3C	33.59	2.95	Different cell arrangement structures and the different locations of the fans	2014	Wang et al. [72]
7	Forced Air-cooling	Air	Square LiFePO4 battery	Numerical	1C	–	–	Inconsistency of battery cells and the positions of the inlet and outlet	2019	Peng et al. [73]
8	Natural convection cooling	Air	18,650 NCM batteries	Numerical + Experiment	2C	34.5	3.1	Different cells distribution strategy to enhance the temperature uniformity	2019	Ji et al. [74]
9	Forced Air-cooling	Air	Battery module	Numerical	–	–	4.1	A comprehensive design optimisation methodology is proposed to improve air cooling performance of a battery module with eight prismatic cells.	2019	Li et al. [75]
10	Forced Air-cooling	Air	18,650 lithium-ion battery	Numerical	5C	37.85	5.5	Orifice diameter, rows of the orifice, the inlet pressure and discharge rate	2019	Zhou et al. [76]
11	Forced Air-cooling	Air	18,650 lithium-ion battery module	Numerical	0.5C/1C	38.9	7.3	Relative positions of air flow inlet and outlet and the utilisation of baffle	2018	E et al. [77]

Please cite this article as: Jiang ZY et al., Recent progress in lithium-ion battery thermal management for a wide range of temperature and abuse conditions, International Journal of Hydrogen Energy, https://doi.org/10.1016/j.ijhydene.2022.01.008

12	Forced Air-cooling	Air	14.6 Ah lithium-ion pouch cell	Numerical	5C	38.9	8.3	Two different configurations of vortex generator: (1) rectangular rib; (2) delta winglet.	2019	Xie et al. [78]
13	Forced Air-cooling	Air	180 Ah prismatic Lithium-ion battery cell	Numerical + Experiment	1C	33.1	–	Two-directional air flow pack	2014	Yu et al. [79]
14	Forced Air-cooling	Air	Prismatic Lithium-polymer battery	Numerical + Experiment	5C	47.4	–	Thickness of the silica cooling plate, air velocity, air inlet position, and number of fans.	2019	Li et al. [80]
15	Forced Air-cooling	Air + Water	Panasonic NCR18650B cylindrical batteries	Experiment	5 A discharges	33.6	6.9	Relative humidity (RH), air flow rate and reciprocating air flow,	2020	Zhao et al. [81]

SEM images of the layered structure are shown in Fig. 3. The battery is fabricated by stacking multiple layers of basic units or winding one basic unit around the centre axis.

The effective thermal conductivity of the LIB is anisotropic due to its layered structure. The thermal conductivity is low along in-plane direction as heat flow through each layer in series, and this results in a lower thermal conductivity. However, the thermal conductivity is high along through-plane direction as heat flow along each layer in parallel, which results in a higher thermal conductivity. It is difficult to calculate the thermal conductivity layer by layer because of the small thickness, and therefore, the battery is modelled as an item with uniform layer structure which has anisotropic thermal conductivity. The thermal conductivity in the perpendicular (in-plane) and parallel directions (through-plane) is calculated as:

$$k_{\parallel} = \frac{\sum k_i s_i}{\sum s_i} \tag{2}$$

$$k_{\perp} = \frac{\sum s_i}{\sum \frac{s_i}{k_i}} \tag{3}$$

The strong anisotropy of battery thermal conductivity has been confirmed in experimental measurements [60]. The in-plane thermal conductivity of LIB has been measured to be 0.15–0.20 W/m·K [61]. The thermal conductivity of typical electrode material is around 2–5 W/m·K [62,63] and the thermal conductivity of typical separator materials is around 0.5–1.0 W/m·K [64], respectively. The thermal conductivity discrepancy of the values calculated using Eq. 2–3 and the measured value is significant [61], which indicates that the interface contact thermal resistance between layers significantly influence the battery thermal behaviour. Nanda et al. [62] investigated the interfacial resistance within a cell unit and found that interfacial resistance contributed to 88% of the total cell resistance. Gaitonde et al. [65] developed a technique for measuring the thermal resistance across a case-separator interface and they found that the thermal conductance through battery case-separator contact interface was 670 ± 275 W/m^{2}K. As mentioned above, the thermal conductivities of different types of batteries (cylindrical, pouch and prismatic cell) are quite different. However, the accurate experimental measurement of thermal conductivity is still difficult, most research obtain the thermal conductivity value via theoretical calculation.

The heat capacity of the battery is determined by both experimental measurements and equivalent calculations by combining each component inside the battery. The average specific heat capacity of the battery can be measured by the ARC. In the measurement, two batteries are required for the prismatic cells, and three or more for the cylindrical cells. As shown in Fig. 4, a “sandwich” structure is built for the measurement, and a controllable heater is placed between the cells. The margins of the cells are sealed with aluminium tape to ensure that the testing battery absorbs all heat produced by the heater. The heat capacity is then calculated using the heating power and temperature increase rate as:

$$c_p = \frac{P}{m\Delta T} \tag{4}$$

Please cite this article as: Jiang ZY et al., Recent progress in lithium-ion battery thermal management for a wide range of temperature and abuse conditions, International Journal of Hydrogen Energy, https://doi.org/10.1016/j.ijhydene.2022.01.008

where P represents the heating power, m denotes the mass of the testing battery, and ΔT represents the temperature increase rate.

Battery cooling method at high operating temperature

Air cooling

The air-cooling system is a mature technique scheme for commercial applications because of its simple configuration and low cost [66]. Some key points such as the battery type used in the study, testing charge/discharge scheme, temperature variation during cooling, and design of the air path need to be considered when referring to the air-cooling research. Table 3 summarises the important features of the recent air-cooling research. For air cooling, firstly, a well-designed configuration of air-cooling is necessary for maintaining temperature uniformity and the temperature range of the battery pack. Further, various methods are proposed to enhance the air-cooling efficiency. Recently, studies on battery air cooling has been focused on optimizing conventional air-cooling structures and proposing a novel cooling structure design.

Pack arrangement, cell spacing, and air path design should be considered for battery pack optimisation. The most important objectives for air cooling design are better temperature uniformity and lower energy consumption. For prismatic LIB, as shown in Fig. 5 (a), the spacing of cells, spacing of the cell and module housing, and location and dimensions of the inlet and outlet are key design parameters. For cylindrical cells, the arrangement of cells should be considered; the most common arrangements include aligned, staggered, and cross structures, as shown in Fig. 5 (b). Chen et al. [67] improved the air-cooling system performance with a Z-type flow and the adjustable cell pacing. The results showed that the maximum cell temperature difference can be reduced by around 60% with optimised cell spacing. Further, they conducted research on the spacing optimisation of an air-cooling system with a U-type air flow [68]. The angles of the plenums and widths of the inlet and outlet were optimised using the nested looped procedure. The power consumption was reduced by 50% with the optimised design. For spacing parameters in the battery pack, Kirad et al. [69] observed that the cooling efficiency factor is prominently affected by the transverse spacing, and the temperature uniformity, by the longitudinal spacing between the batteries. For cell arrangement, Fan et al. [70] investigated the air cooling performances of aligned, staggered, and cross battery packs and found that the aligned arrangement had the

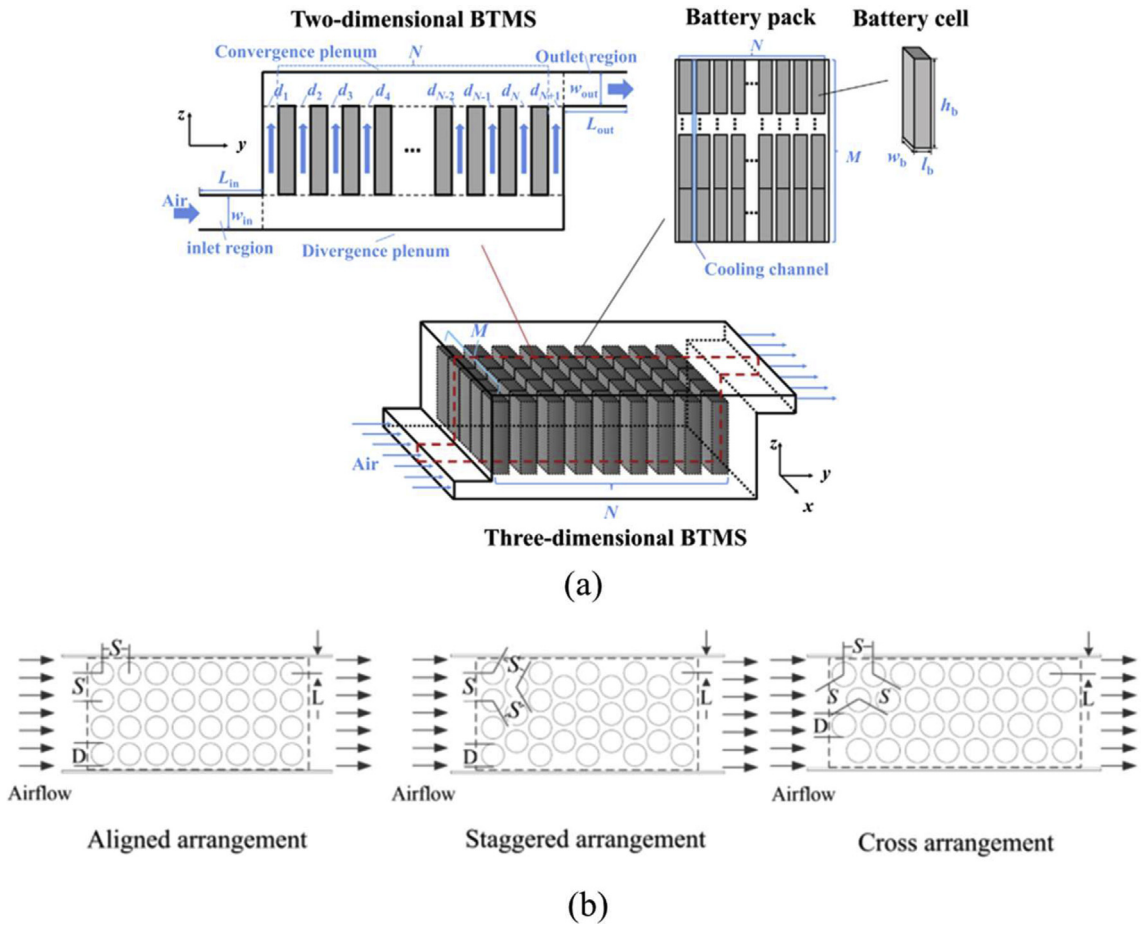

Fig. 5 – Cell spacing and arrangement design of air-cooling structure. (a) key spacing parameters in battery pack [68]; (b) three cell arrangements [70].

Please cite this article as: Jiang ZY et al., Recent progress in lithium-ion battery thermal management for a wide range of temperature and abuse conditions, International Journal of Hydrogen Energy, https://doi.org/10.1016/j.ijhydene.2022.01.008

best cooling performance and temperature uniformity; further, they found that the temperature difference was reduced by 12% compared with those for the cross arrangement. A poor temperature uniformity is observed along the air flow direction, although more fierce air turbulence is achieved in the stagger and cross arrangement. Compared with the battery arrangement, the air inflow velocity was more predominant for the cooling performance. In addition to the arrangement of single cells in a battery pack, the locations of the inlet and outlet of the cooling medium need to be investigated in an air-cooling system. Lu et al. [71] investigated the effects of the cooling channel size and air supply strategy on the stagger-arranged thermal behaviour of the battery pack. They used a novel internal air passage inlet, and the best cooling performance was achieved when the airflow inlet and outlet were located at the top of the battery pack. Wang et al. [72] investigated the thermal performance of a battery module with different pack structures. The best cooling performance was achieved when the fan was located at the top of the module. Peng et al. [73] considered the inconsistency of the cells in the pack and proposed a more realistic thermal model of the battery pack at a 1C discharge rate through equivalent calculation and experimental verification. They proved that cooling performance could be improved by placing the inlet and outlet on the same side because the maximum temperature was reduced with a longer air path. Ji et al. [74] designed a different cell distribution strategy to enhance temperature uniformity in a cylindrical battery pack module. It was confirmed that varying the spacing can efficiently improve the temperature uniformity. A structure optimisation method considering cell arrangement and spacing was also implemented. Li et al. [75] proposed a comprehensive 4 step methodology to optimise the volume and cooling performance of air-cooling system. The optimised air-cooling system showed a higher thermal performance by using the multi-objective optimisation approach.

For present air-cooling system, the heating efficiency is still not enough for the large format power battery module. Therefore, in addition to structure optimisation, novel heat transfer enhancement designs are introduced to improve the cooling performance of air-cooling systems. The primary goals of designing a new air-cooling structure include: i) achieving a more uniform air flow in the battery pack for temperature uniformity and ii) increase turbulence in the air path for a high heat exchange coefficient. Fig. 6 shows some unconventional air-cooling structures of the battery pack. As indicated in Fig. 6 (a), Zhou et al. [76] used an air distribution pipe for the cooling of cylindrical LIBs. The cooling structure decreases the module temperature by 20 °C. E et al. [77] used a baffle to improve cooling efficiency in air-cooling system and they found that the use of the baffle plate significantly improves the cooling performance with the lateral inlet and outlet. Xie et al. [78] introduced a vertex generator in the air flow path of an air-cooling system. The battery temperature

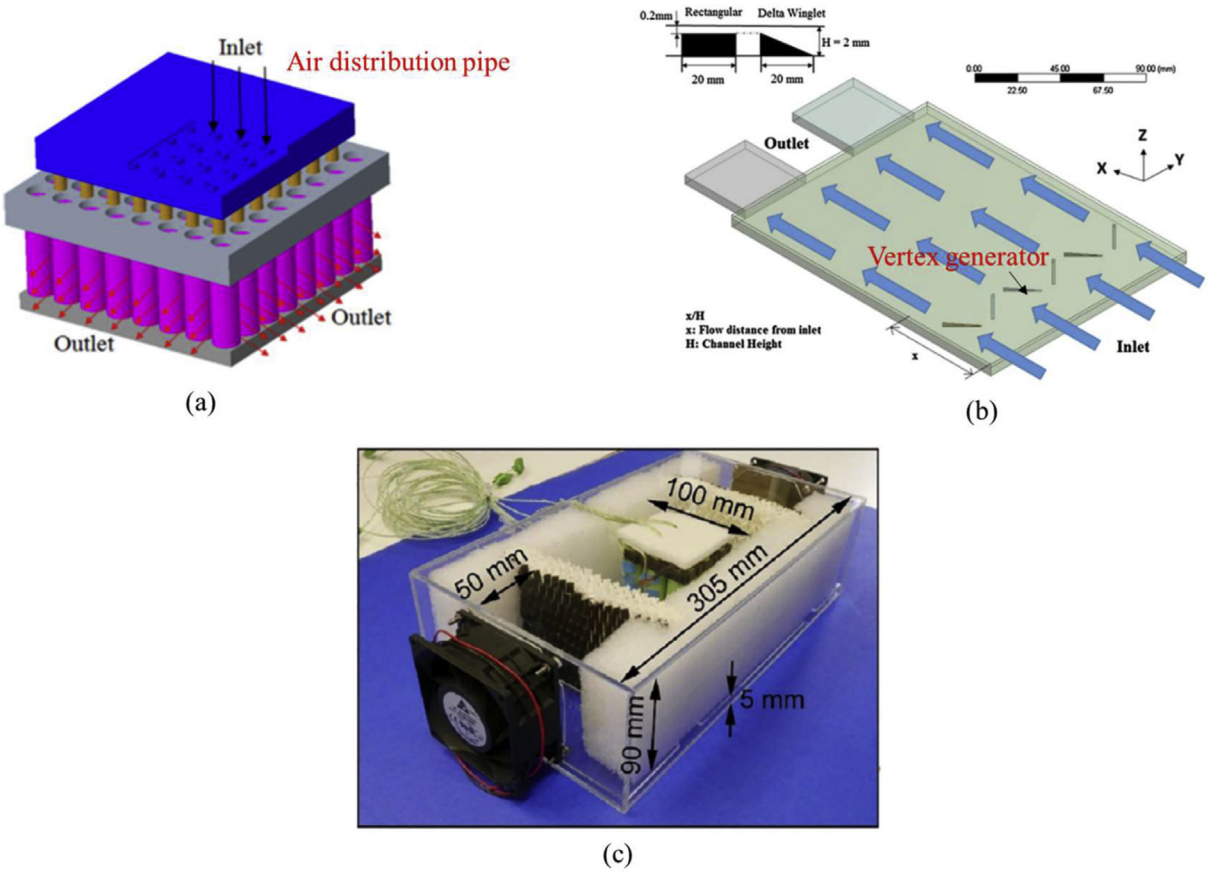

Fig. 6 – Methods to improve the cooling efficiency in air cooling. (a) Cooling structure with an air distribution pipe [76]; (b) cooling structure with vertex generator [78]; (c) cooling structure combined with evaporative cooling module [81].

Please cite this article as: Jiang ZY et al., Recent progress in lithium-ion battery thermal management for a wide range of temperature and abuse conditions, International Journal of Hydrogen Energy, https://doi.org/10.1016/j.ijhydene.2022.01.008

Table 4 – Summary of recent developments in liquid-cooled BTMS.

No.	Cooling system	Heat transfer coolant	Battery type	Type of study	Battery load	T_{max} (°C)	ΔT_{max} (°C)	Variables/Remarks	Year	References
1	Liquid cooling with tubes	Water	18,650 cylindrical lithium-ion battery module	Experiment	3C	42.0	4.0–5.0	Water cooling battery module with GO-SG(graphene-oxide-modified silica gel) shows excellent cooling performance.	2019	Lv et al. [85]
2	Liquid cooling	Galden HT135, Silicone oil	$LiNi_yMn_yCo_{1-2y}O_2$ and $LiFePO_4$ batteries	Experiment	–	–	–	Two experimental rigs have been set up to test the capability of different cooling fluids with different types of batteries.	2019	Menale et al. [86]
3	Liquid cooling with tubes	Water, liquid metal(Ga^{80} In^{20}).	$LiFePO_4$ (LFP) lithium-ion battery	Numerical	5C	<40	<5	Type of coolant, flow velocity, number of copper pipes, discharge rate	2020	Liu et al. [87]
4	Liquid cooling with half-helical duct	Water	Cylindrical 18,650 lithium-ion battery	Numerical	5C	30.9	4.3	A novel cooling strategy based on the half-helical duct and a three-dimensional computational fluid dynamics model are proposed.	2019	Zhou et al. [88]
5	Liquid cooling with aluminum block	Water	SONY cylindrical 26,650 lithium-ion battery	Numerical	3C	<40	–	Types of contact surface, inlet velocity, aluminum block length, pump power consumption	2017	Rao et al. [89]
6	Liquid cooling with cooling plate	Mixture of water and glycol	49 Ah prismatic lithium-ion battery	Numerical + Experiment	1.2C	38.39	<5.31	A liquid cooling system with changing contact surface is proposed and three factors (mass flow rate, inlet temperature, the width of cooling plate) are optimised.	2019	Shang et al. [90]
7	Liquid cooling with mini-channel plate	Water	20 Ah capacity lithium-ion pouch type battery	Numerical + Experiment	1C, 2C	–	–	New cooling structure with the "zig-zag turn" type aluminum mini-channel cold plates is proposed.	2017	Panchal et al. [91]
8	Liquid cooling with flow boiling	NOVEC 7000 coolant	20 Ah prismatic $LiFePO_4$ power batteries	Experiment	1C, 3C, 5C	36.6 (5C)	–	A new type of BTMS based on flow boiling in mini-channel utilizing dielectric hydrofluoroether liquid is proposed.	2017	An et al. [92]
9	Liquid cooling with channels	Water	18,650 cylindrical lithium battery	Numerical	5C	<39.85	<3.15	Number of channel, hole diameter, mass flow rate and inlet locations	2021	Yates et al. [93]
10	Liquid cooling with cold plate	Water	Rectangular lithium ion batteries	Numerical	5C	31.18	1.15	Mass flow rate of cooling liquid, cold plate number, channel distribution and cooling direction	2019	Deng et al. [94]
11	Liquid cooling with cooling plate	Water	30 Ah pouch $LiFePO_4$ lithium-ion battery	Numerical + Experiment	0.5C, 1C, 2C	32 (2C)	6.2 (2C)	Inlet flow rate, the cooling channel size, the discharge rate	2020	Du et al. [95]
12	Jacket liquid cooling	Water	70 Ah prismatic $LiFePO_4$ lithium-ion battery	Numerical	1C	32.5	1.5	A novel BTMS consisting of a cover plate to uniformly distribute water in different cold plates is proposed.	2019	Xu et al. [96]

Please cite this article as: Jiang ZY et al., Recent progress in lithium-ion battery thermal management for a wide range of temperature and abuse conditions, International Journal of Hydrogen Energy, https://doi.org/10.1016/j.ijhydene.2022.01.008

13	Liquid cooling with cold plate	Water	3.65 V/20 Ah prismatic Li-ion battery	Numerical	5C	41.92	1.78	Single battery cell and large scale numerical simulation with silicon cold plates coupled with copper tubes is studied.	2019	Li et al. [97]
14	Mini-channel liquid cooling + air cooling	Air + Water	2.0 Ah cylindrical 18,650 Li-ion battery	Numerical + Experiment	4C	39.0	4.4	Water inlet flow rate, the amount of cooling tube and mini-channel, water flow direction, the combination of different spacer, air inlet velocity	2020	Yang et al. [98]
15	Liquid cooling with mini-channels	Water-ethylene glycol mix	Rectangular lithium-ion battery	Numerical	–	–	–	Novel cooling structure with the typical and streamline shape mini-channel is proposed.	2019	Huang et al. [99]
16	Jacket liquid cooling	Water	8 Ah lithium-ion soft-pack battery	Numerical + Experiment	1C	<32.8	<2	Multi-Objective optimisation of micro-channel in coling plate is proposed.	2019	Chen et al. [100]
17	Liquid cooling with tubes	Water	5.0 Ah cylindrical 26,650 Li-ion battery	Experiment	1C, 1.5C	31.8 (1C)	4.2 (1C)	Active liquid cooling system with mini-channel under different cooling schemes is investigated.	2018	Du et al. [101]
18	Immersion cooling	Water	18,650-type lithium-ion power battery	Experiment	3C	<35	<0.5	Battery coated with silicone sealant/BN composite materials is directly immersed in water to dissipate heat.	2020	Li et al. [102]

can be decreased by 10%, and the local Nusselt number can be enhanced by 38% compared to that without a vertex generator at 5C discharge (Fig. 6 (b)). Heat transfer enhancement in the cooling structure is attributed to bulk fluid mixing, boundary layer modification, and flow destabilisation by the vertex generator. Yu et al. [79] proposed an air-flow-integrated cooling structure to minimise battery temperature differences in LIB pack. The results indicate that the maximum temperature can be decreased by around 8 °C with the integrated structure in comparison with traditional systems. Li et al. [80] proposed a cooling structure using a double-silica cooling plate and a copper mesh and they found that the battery temperature can be controlled under 50 °C with 5C discharge rate. Recently, Zhao et al. [81] proposed a new approach for air-cooling enhancement (Fig. 6 (c)). The cooling system is improved by incorporating a direct evaporative cooling (DEC) system. The evaporation section is fixed at the inlet of the air tunnel, which reduces the air temperature at inlet. Results show that the DEC tunnel can produce reciprocating airflow that can further enhance the heat exchange in the cooling system.

Liquid cooling

The liquid cooling is more efficient cooling method compared with air cooling, but the liquid cooling system is more complex than air-cooling and suffers the risk of leakage of liquid working fluid. The typical liquid cooling can be by achieved by equipping discrete tubing or ribbon-shaped metallic heat exchangers around each cell [82], while placing the cells on a liquid heated/cooled plate (heat sink) [83,84]. Table 4 summarises the latest liquid cooling-based research on the BTMS.

Recently, battery liquid cooling studies have focused on proposing a highly efficient working fluid, optimizing the flow structure, and utilizing a cooling plate with a mini-channel. For the working fluid, a novel fluid with higher thermal conductivity and stability is flavoured in the liquid cooling system design. Lv et al. [85] prepared graphene oxide-modified silica gel (GO-SG) and filled it in the space between the cylindrical cells and water-cooling tubes. The insertion of GO-SG improves the thermal conductivity of the module, and the generated heat is transferred to the cooling tube more efficiently. The temperature difference in LIB pack is controlled below 4 °C with GO-SG. The increment of fluid thermal conductivity enables the system to achieve the same cooling performance at a lower flow rate, which can reduce system energy consumption. Menale et al. [86] tested the cooling capabilities of various cooling fluids. The experimental results show that air cannot limit the surface temperature increase; the perfluorinated polyether fluid can maintain the battery temperature within the optimal temperature range, even under severe operating conditions. In addition to conventional coolants such as water and silica gel, liquid metal is introduced as a liquid cooling strategy. Liu et al. [87] utilised a liquid metal composed of $Ga^{80}In^{20}$ to enhance the liquid cooling performance of a LiFP battery. Results show that liquid metal can be used under extreme conditions. However, the utilisation of liquid metal in BTMS remains in the numerical simulation, and the experimental exploration is necessary to verify the effectiveness of the liquid metal.

Please cite this article as: Jiang ZY et al., Recent progress in lithium-ion battery thermal management for a wide range of temperature and abuse conditions, International Journal of Hydrogen Energy, https://doi.org/10.1016/j.ijhydene.2022.01.008

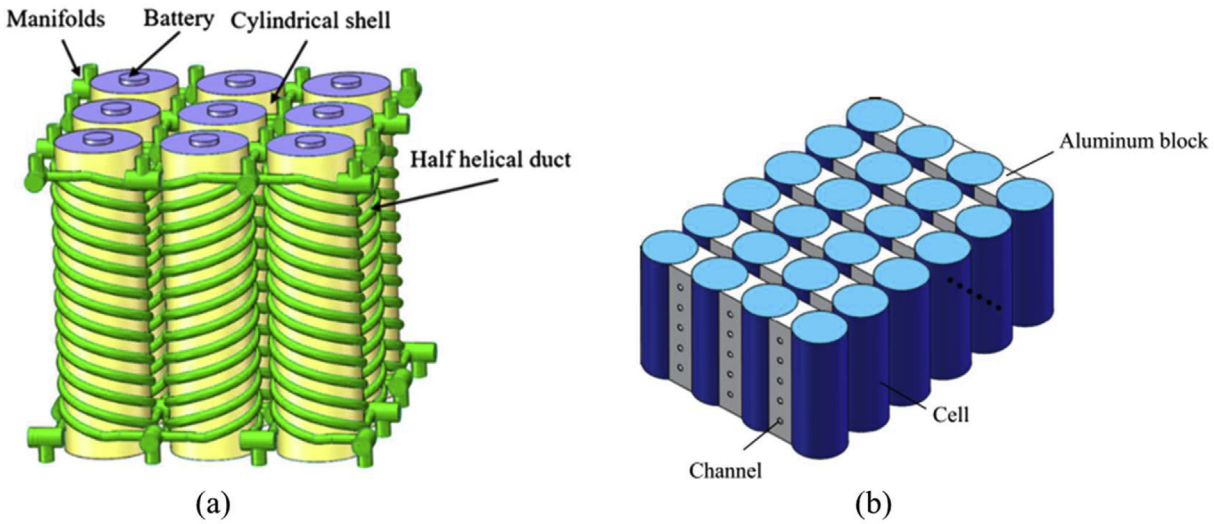

Fig. 7 – Design of contact surface between cooling pipe and battery: (a) contact using half-helical duct [88]; (b) contact using aluminium block with curved surface [89].

A critical issue in liquid cooling includes the poor contact between the battery surface and cooling liquid duct. Therefore, it is critical to design a proper contact surface to reduce the thermal resistance of the liquid cooling structure. Zhou et al. [88] proposed a liquid cooling method based on a half-helical duct, as indicated in Fig. 7 (a). Compared to thermal management using the jacket liquid cooling method, that using the half-helical duct is more efficient due to the low fluid

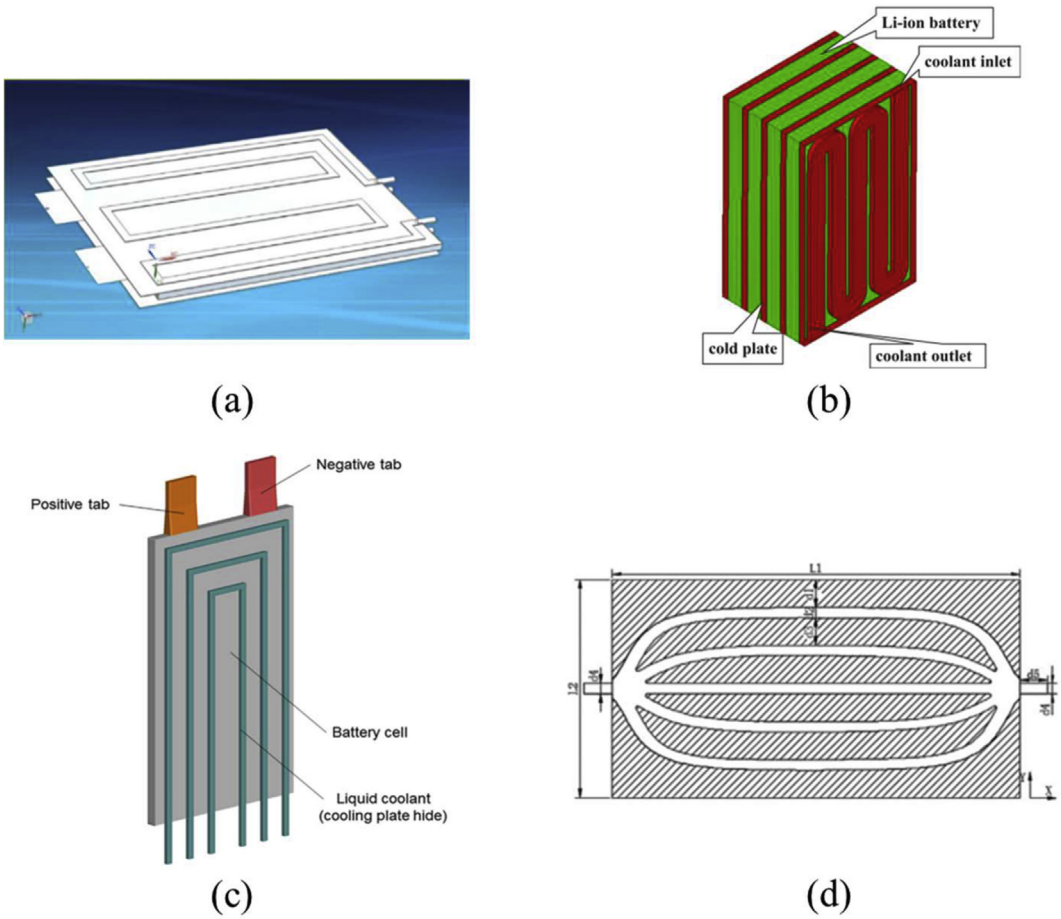

Fig. 8 – Typical design of cold plate: (a) zig-zag turn structure [91]; (b) serpentine flow field structure [94]; (c) rectangular-ambulatory plane [97]; (d) optimised streamline structure [99].

Please cite this article as: Jiang ZY et al., Recent progress in lithium-ion battery thermal management for a wide range of temperature and abuse conditions, International Journal of Hydrogen Energy, https://doi.org/10.1016/j.ijhydene.2022.01.008

Table 5 – Summary of recent developments in the PCM cooling BTMS.

No.	Cooling system	Phase change material	Battery type	Type of study	Battery load	T_{max} (°C)	ΔT_{max} (°C)	Variables/Remarks	Year	References
1	PCM cooling	graphite matrixes	2.2 Ah cylindrical 18,650 Li-ion battery	Experiment	2.08C	<45	4	Passive thermal management system using graphite matrixes for lithium-ion batteries is tested.	2008	Kizilel et al. [103]
2	PCM cooling (Al-foam)	–	2.2 Ah cylindrical 18,650 Li-ion battery	Experiment + Numerical	1C, 0.5C, 0.2C	22 (1C)	2.5	Battery pack with PCM distributed in the pores of aluminum foam is tested.	2005	Khateeb et al. [104]
3	PCM cooling	–	8 Ah ageing rectangular $LiFePO_4$ power batteries	Numerical + Experiment	5C	<50	4.94	PCM with low melting point can make the maximum temperature of battery pack below 50 °C.	2011	Rao et al. [105]
4	PCM cooling	flexible CPCM	Cylindrical 18,650 lithium-ion battery	Numerical + Experiment	10C	55	1.9	Phase change temperature of flexible CPCMs, working condition, the ambient temperature	2019	Huang et al. [118]
5	PCM cooling	paraffin, graphite, epoxy resin	Nine 18,650 lithium-ion batteries	Experiment	4C	33	1.4	Battery pack with a novel PCM composites coupled with graphite film is tested.	2020	Luo et al. [119]
6	PCM cooling	C-PCM	NCR18650-GA lithium-ion batteries	Experiment	1C, 2C	42.8 (2C)	4.7 (2C)	Novel BTMS based on C-PCM consisting of 5 wt% of expanded graphite and 95 wt% of paraffin with aluminum boxes is tested.	2018	Wang et al. [120]
7	PCM cooling	trimethylolethane hydrate	18,650 lithium-ion battery	Experiment	–	–	–	Best concentration may be $w_{TME} = 0.60$ as the largest dissociation heat 190.1 kJ/kg is available	2019	Koyama et al. [121]
8	Mist cooling	water	8 Ah 38,120 lithium iron phosphate battery	Numerical + Experiment	1C, 2C, 3C	<40	–	Mass flow rate, the charge/discharge rate, the mist loading fraction	2018	Saw et al. [108]
9	Evaporative cooling	water	94 Ah prismatic lithium iron battery	Experiment	250 A	34.5	–	Battery pack with thin sodium alginate film (SA-1 film) under different condition is investigated.	2017	Ren et al. [107]
10	PCM cooling + liquid cooling	paraffin + graphite matrix	40 Ah rectangular $LiFePO_4$ battery	Numerical	2C	27.4	3.87	Refrigerant-cooled BTMS, conventional PCM based passive BTMS	2019	Park et al. [122]

Please cite this article as: Jiang ZY et al., Recent progress in lithium-ion battery thermal management for a wide range of temperature and abuse conditions, International Journal of Hydrogen Energy, https://doi.org/10.1016/j.ijhydene.2022.01.008

volume and the missing stagnant zone. To improve the surface temperature uniformity, Rao et al. [89] designed a novel cooling system with a variable contact surface as illustrated in Fig. 7 (b). Results show that the maximum battery temperature in the system is controlled under 40 °C with the variable contact surface structure. Shang et al. [90] designed a LIB liquid cooling system with a changing contact surface. The results indicate that the battery temperature in the test is proportional to the inlet temperature and is inversely proportional to the cooling plate width.

Considerable attention has been paid to cold plates with mini-channels because of their feasible application and high heat transfer efficiency to enhance the cooling efficiency of liquid cooling. Most investigations focused on the optimisation of the cold plate geometry and operation parameters. The channel configuration, channel size, channel number, inlet flow rate, and location of the inlet and outlet are the most important parameters. Typical designs of the cold plate are summarised in Fig. 8. Panchal et al. [91] investigated cooling performance of the zigzag turn-type aluminium mini-channel cold plates, as indicated in Fig. 8 (a). An et al. [92] proposed a novel mini-channel with flow boiling for LIB. The dielectric hydrofluoroether liquid was used as working fluid. Results show that the boiling cooling can significantly decrease the maximum battery temperature and temperature difference. Yates et al. [93] compared the performance of a mini channel-cooled cylinder (MCC) and a channel-cooled heat sink. Despite the manufacturing cost, the performance of MCC design is better with lower battery temperature and temperature difference. Deng et al. [94] constructed a liquid cooling battery pack using a "sandwich" structure design, as shown in Fig. 8 (b). The effects of the mass flow of the cooling liquid and cold plate number on the cooling performance of the battery pack are evaluated. The optimum mass flow rate and reasonable cooling direction are determined. Du et al. [95] discussed the cooling of a $LiFePO_4$ pouch battery pack with a cooling plate. They found that the inlet flow rate and cooling channel size significantly influenced the battery charging process. They reported that the proper flow rate should be selected for the cooling plate; a rate larger than 0.5 m/s saturates the cooling effect. In addition to the optimisation of the channel geometry, the bifurcation structure is important for enhancing the mini-channel performance. Xu et al. [96] proposed an improved water-cooling system using two novel cover plates with T-shaped bifurcation structures. The cold plate can efficiently spread the battery heat to the coolant, but the conduction of heat from the mini-channel to the environment is also important. Therefore, a coupling structure is necessary to improve the overall performance of the cold plate. Li et al. [97] proposed a novel cooling structure that consists of as-constructed silicon cold plates coupled with copper tubes, as shown in Fig. 8 (c). In this new design, the generated heat is transferred to the copper tubes efficiently via the silicon cold plate; the heat can be efficiently dissipated by the water flow through the copper tubes. The proposed cooling system can control the maximum battery temperature below 41.92 °C and the temperature difference within 1.78 °C with a small liquid flow rate of 8 ml/s. Further, air cooling was introduced in the cold plate cooling structure. Yang et al. [98] proposed a combined cooling structure of air cooling and mini-channel liquid cooling to overcome the temperature increment along the flow direction of the coolant. Most cold plates utilise the straight channel, and the turbulence and flow resistance are likely to increase in rectangular areas. Therefore, a streamline channel shape is introduced in the channel design to reduce the flow resistance. Huang et al. [99] proposed a novel design method of mini-channel cold plate using a streamline shape concept, as shown in Fig. 8 (d). The designed flow channel can increase the cooling performance by 44.52%.

The research on system optimisation was conducted in the liquid cooling design. Chen et al. [100] employed the multi-objective optimisation for liquid cooling design. The results indicate that the battery temperature is decreased by 1.87 °C and the temperature difference is controlled within 0.35 °C in the optimised cooling system. Du et al. [101] investigated the optimisation of liquid cooling system control. The results showed that a simple hysteresis control can reduce the energy consumption by 83.2% at 1C rate.

Most liquid cooling uses an indirect structure, which indicates that the coolant must be contained in the cooling duct. However, cooling efficiency improves significantly if a battery module can be directly immersed in water to dissipate heat. The critical issue in this immersion BTMS structure is the waterproof treatment of the battery surface. Recently, Li et al. [102] proposed an immersion cooling strategy by immersing the battery into a water bath. The surface of the battery was coated with a silicone sealant/BN composite material. The

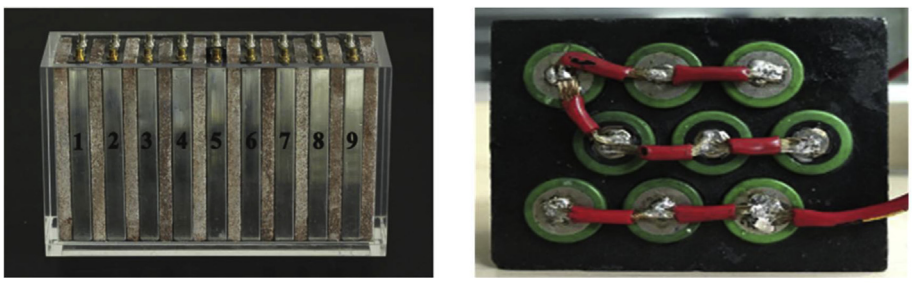

(a) (b)

Fig. 9 – Illustration of various PCM cooling structure: (a) PCM and copper foam composite [111]; (b) PCM/Expanded graphite/Epoxy resin composite [119].

Please cite this article as: Jiang ZY et al., Recent progress in lithium-ion battery thermal management for a wide range of temperature and abuse conditions, International Journal of Hydrogen Energy, https://doi.org/10.1016/j.ijhydene.2022.01.008

immersion cooling showed excellent cooling performance, and the maximum temperature of the LIB module was controlled at 35 °C during 3C cycle.

Cooling with phase change material

The PCMs can absorb and release abundant latent heat and is used as an efficient thermal control medium in battery BTMS. The PCM used in the cooling system can be categorised as solid–liquid phase change [103–105] and gas–liquid phase change materials [106–108]. Table 5 summarises the PCM-based research on BTMSs in recent years.

Solid–liquid PCMs are commonly used in passive BTMS, and the liquid PCMs are commonly used in active BTMS. The LIB pack can perform efficiently with lower temperature and temperature different at extreme cycling conditions [103]. However, the cooling performance of PCM is limited by its low thermal conductivity [109], and therefore, enhancing the thermal conductivity of the PCM is critical for PCM applications in BTMS. Generally, the thermal conductivity of PCM can be increased by introducing high thermal conductive additives such as aluminium wire [110], metal foam [111–114], carbon fibre [115,116], and graphite [117], as shown in Fig. 9. In addition, novel strategies that can enhance the thermal conductivity of PCMs in passive BTMS have been proposed. Huang et al. [118] proposed a flexible form-stable composite phase change material (CPCM) for battery temperature control. The flexible CPCMs can reduce the contact thermal resistance and can enhance its cooling performance in the battery module. The battery temperature was reduced by 18 °C at a 10C discharge. Luo et al. [119] designed a novel phase change material consisting of paraffin with dual-phase transition ranges, expanded graphite, and epoxy resin. Experimental results showed that the maximum temperature difference is around 1.4 °C at a 4C discharge. Wang et al. [120] proposed a novel battery-cooling structure based on a CPCM with aluminium boxes. The experimental results showed that C-PCM reduced the average battery temperature and temperature difference. A new PCM with better thermal performance was introduced instead of using paraffin as the PCM. Koyama et al. [121] employed trimethylolethane (TME) hydrate as the PCM in a battery cooling system. The hydrate has a large dissociation heat and a low melting temperature at around 30 °C. The cooling capability of the TME material was three times greater than that of liquid water.

Liquid–gas phase change processes such as mist, water spray, and refrigerant evaporation have been introduced in the BTMS instead of using solid–liquid phase change heat transfer process. Saw et al. [108] proposed a mist cooling strategy for battery cooling and results showed that mist cooling can keep the LIB pack at lower temperature and temperature difference compared with dry air cooling. Ren et al. [107] proposed a water spraying cooling strategy based on a sodium alginate film with water content at 99 wt%. The temperature rise rate was decreased by 50% with a current rate larger than 1C. Park et al. [122] investigated the refrigerant-cooled BTMS. The cooling performance of the refrigerant-cooled BTMS was compared with that of conventional PCM-based passive BTMS. The refrigerant-cooled active BTMS showed better cooling performance during the battery cycling test. Recently, the desorption/adsorption heat of liquid in porous medium has been adopted as a thermal management pathway with the advantages of no energy consumption and wide range temperature control [123]. Xu et al. [124] propose a near-zero-energy battery thermal management strategy for both passive heating and cooling based on the thermal effect of water desorption/adsorption in metal-organic framework. The proposed method can control the battery temperature below 45 °C in hot environment.

Active and passive combined cooling method

The BTMS with a single cooling strategy is insufficient to compromise the cooling performance, the combined cooling methods are therefore proposed. Most combined cooling methods used a PCM as passive cooling part and an air or liquid cooling as active cooling part. Table 6 summarises the active and passive combined cooling methods in recent years. One important issue for combined cooling system is connecting the active and passive cooling with an efficient thermal connection device. Heat pipes (HPs) have been widely utilised as a highly efficient thermal connection device in temperature control technique in recent years [125–127].

The application of HPs in LIB thermal management has been well approved [128,129]. Tran et al. [130] conducted experiments on the cooling performance of HPs used in cylindrical LIB pack, which is shown in Fig. 10(a). Results show that the HP can reduce the contact thermal resistance by 30% in BTMS. Ye et al. [131,132] investigated the cooling performance of HP with air cooling at its cooling end, which is shown in Fig. 10(b). Results show that the efficiency of HP at its cooling end is critical in HP application. Further, Zhao et al. [133] tested the performance of HP with different cooling methods, natural and forced convection and spray cooling, on its cooling end, as shown in Fig. 10(c). Water spray was found to be the optimum approach among proposed methods. Wang et al. [134] used an L-type heat pipe (Fig. 10(d)) for battery cooling, and the cooling end of the heat pipe was immersed in a glycol-water coolant. Results show that the battery temperature could be maintained at 41.1 °C under 4C discharge.

A micro heat pipe array (MHPA) structure was introduced in the BTMS to fully exploit the advantages of heat pipe cooling. Compared to a conventional heat pipe, the MHPA can reduce the contact thermal resistance due to the smaller size. Ye et al. [135] designed a BTMS based on the MHPAs. The cooling structure can minimise the temperature difference inside the LIB packs when coupled with forced air convection outside the pack. Dan et al. [136] conducted numerical simulations for an air-cooled MHPA cooling system based on a thermal network model. Their results showed that the MHPA-based cooling structure could provide a quick response to rapidly changing operating conditions.

The storage of PCM in BTMS is limited considering the energy density of the battery power system. The heat accumulation in PCM induces the exhaustion of its latent heat and causes overheat of the battery. Therefore, the combine cooling methods is proposed due to the fact that the single PCM is not sufficient to control the battery temperature in a long-time range. Ling et al. [137] compared cooling performances of PCM and PCM combined with forced air convection. They

Please cite this article as: Jiang ZY et al., Recent progress in lithium-ion battery thermal management for a wide range of temperature and abuse conditions, International Journal of Hydrogen Energy, https://doi.org/10.1016/j.ijhydene.2022.01.008

Table 6 – Summary of recent development of cooling BTMS with combined cooling.

No.	Cooling system	Heat transfer coolant	Battery type	Type of study	Battery load	T_{max} (°C)	ΔT_{max} (°C)	Variables/Remarks	Year	References
1	HP + air cooling	Air	7 Ah cylindrical lithium iron battery	Experiment	–	<50	–	Battery module with heat sink and heat pipe under different condition is investigated.	2014	Tran et al. [130]
2	HP + air cooling	Air/water	10 Ah prismatic LIBs (140 × 65 × 15 mm)	Numerical + Experiment	8C	25–40	<5	Cooper heat spreaders and cooling fins	2016	Ye et al. [131,132]
3	HP + air/wet cooling	Air/water	3 Ah and 8 Ah lithium ion battery	Experiment	1C, 2C, 3C	<32 (3C)	<2.5 (3C)	BTMS combined heat pipe and wet cooling, lengths, and different condition of cooling ends	2015	Zhao et al. [133]
4	HP + liquid cooling	Glycol-water	Simulated battery containers	Experiment	1–4 C	<40	–	Battery cooling, battery preheating (cartridge heaters), L-type heat pipe	2015	Wang et al. [134]
5	HP + forced air cooling	Air	18 Ah prismatic $LiFePO_4$ battery	Experiment	1C	25–40	<5	Micro heat pipe arrays (MHPAs) structure, fins and fan, the discharge rate, forced convection air cooling	2018	Ye et al. [135]
6	HP + forced air cooling	Air	55 Ah prismatic Li-ion battery	Numerical + Experiment	1C, 2C, 3C	<40	<2	Air velocity, the discharge rate, different ambient temperature, micro heat pipe arrays (MHPAs)	2019	Dan et al. [136]
7	PCM + forced air cooling	RT44HC + air	Twenty 18,650 2.6 Ah Li-ion batteries	Numerical	1.5C, 1C	<50	–	Combined cooling system that integrates PCMs with forced air convection is presented.	2015	Ling et al. [137]
8	HP + PCM cooling	Paraffin wax/ CLOHP	Simulated battery containers	Experiment	10–80 W	–	–	Simulated battery with paraffin wax and CLOHP under different supplied heating power (10–80 W) is investigated.	2016	Zhao et al. [138]
9	HP + PCM + air cooling	PCMPs/HP (sintered copper-water)/air	12 Ah prismatic Li-ion batteries	Experiment	1C, 3C, 5C	<50 (5C)	–	Different condition (No PCM, the PCMP and the HP-PCMP), discharge rates, forced air flow, cycle test	2017	Wu et al. [139]
10	HP + PCM cooling	Paraffin wax/ EG mixture	8 Ah LiFePO4 prismatic lithium-ion battery	Numerical + Experiment	3C	<50	0.8	Coupled sandwich cooling structure consisting of a battery, phase change material, and heat pipe is proposed.	2019	Jiang et al. [140]
11	PCM + liquid cooling	PCM/ EG + water	2.6 Ah type 18,650 Li-ion batteries	Numerical + Experiment	1.5C	<37	<3	Weight and volume of PCM, flow rate of water	2018	Ling et al. [141]

Please cite this article as: Jiang ZY et al., Recent progress in lithium-ion battery thermal management for a wide range of temperature and abuse conditions, International Journal of Hydrogen Energy, https://doi.org/10.1016/j.ijhydene.2022.01.008

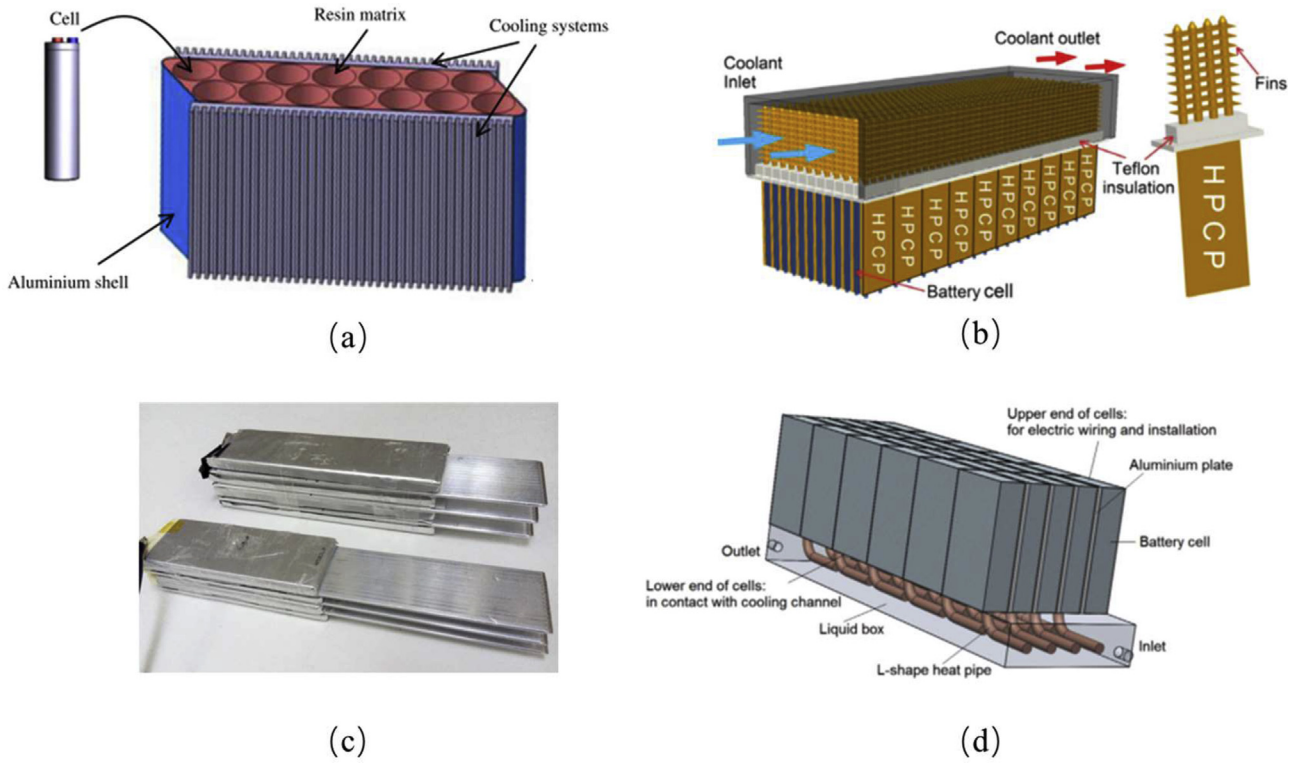

Fig. 10 – Illustration of various heat pipe cooling structure: (a) flat heat pipe with natural convection [130]; (b) tube heat pipe with forced air cooling [132]; (c) flat heat pipe with water spray [133]; (d) tube heat pipe with liquid cooling [134].

found that the PCM can only maintain the battery temperature in a few cycles due to its limited latent heat storage. Therefore, a combination of passive PCM-based BTMS and active air-or liquid-based active BTMS is proposed to maintain the performance of cooling system during long-term cycles, as shown in Fig. 11. In most investigations [142,143], the coupling system is composed of a PCM, heat pipe, and forced air outside the module. The HP is able to amplify the efficient working range of the PCM, which can improve the overall cooling effect of BTMS in the coupling cooling system [144]. Zhao et al. [138] conducted an experimental research on the performance of a BTMS composed of paraffin wax and the closed-loop oscillating heat pipe (CLOHP). The paraffin wax/CLOHP coupling structure is proved to own better cooling capability than the paraffin wax. Wu et al. [139] proposed an HP-assisted PCM cooling system which is shown in Fig. 11(a). The thermal conductivity of PCM is enhanced by mixing with expanded graphite (EG) composite. Results showed that the HP-assisted PCM/EG composite could decrease the battery temperature and temperature difference in LIB pack. As shown in Fig. 11(b), Jiang et al. [140] designed a coupled sandwich cooling structure that comprised a battery, PCM, and heat pipe. They conducted a comprehensive investigation of the temperature response and underlying heat transfer mechanism of the cooling structure. The study showed that the insertion of a heat pipe can increase the working range of the PCM in the cooling module. Ling et al. [141] developed an optimisation method based on the response surface methodology to minimise the weight and volume of the PCM and liquid cooling coupled BTMS. The effects of the battery pack layout, PCM composite, and cooling intensity are discussed. The mass and volume of the PCM were reduced by 94.1% and 55.6%, respectively, after optimisation.

Battery heating at sub-zero temperature

LIBs suffer from poor performance at low temperatures. The slowdown of charge transfer and electrochemical reaction in LIB electrode increase the polarization, which decreases the output performance of LIB. Moreover, charging the battery at low temperature induces the lithium plating which induces the capacity loss by hindering the intercalation of lithium between the anode and electrolyte [145]. The plated lithium reacts with the electrolyte, which induces the loss of lithium-ion and accelerates capacity loss. Therefore, the LIB should be preheated prior to use to maintain a normal start-up and adequate energy output when used in low temperature environment. Battery heating can be realized by applying both an external heat source and an internal heat source. Table 7 illustrates the preheating research in recent years.

External heating methods

The most common heating method involves heating the battery with an external heating source. The heat source can be a hot fluid (air or liquid) that blows the battery or a heating medium wrapping the battery. The air heating method is the easiest method for external heating owing to its feasibility. Li et al. [146] proposed the heating method using positive

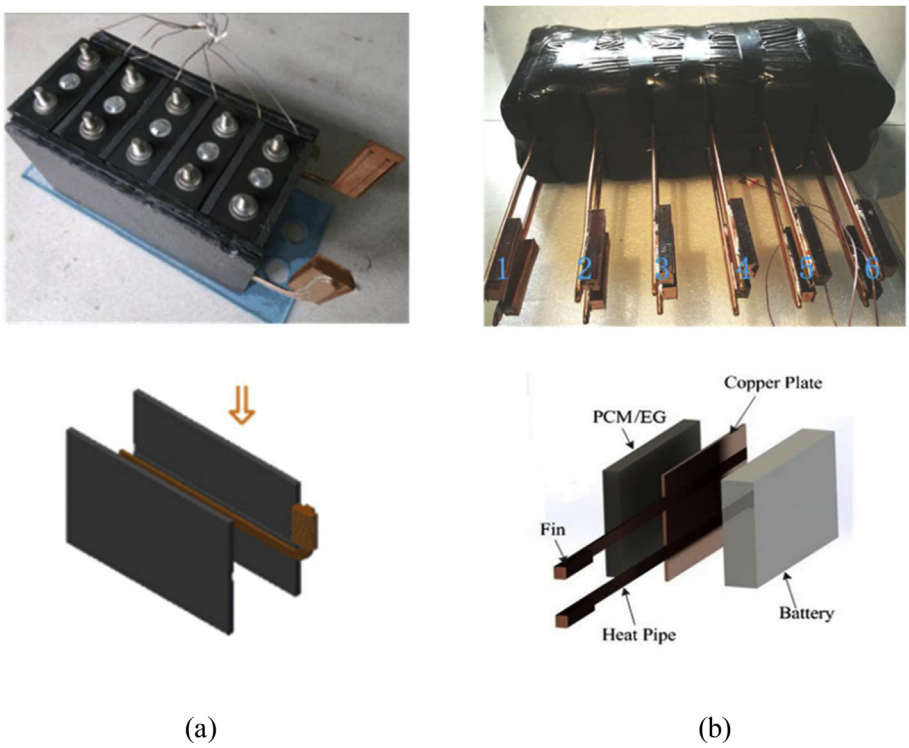

Fig. 11 – Illustration of heat pipe and PCM coupled cooling structure: (a) L-type heat pipe and PCM [139]; (b) heat pipe and PCM sandwich structure [140].

temperature coefficient (PTC) resistance and found that the battery capacity increased from 21.9 Ah to 24.11 Ah with adequate heating power. Pesaran et al. [147] warmed the LIB with the external air convection and found that the 20 °C increment could be achieved for battery within 300 s with a 4.71 Wh heating power input. Song et al. [148] also conducted battery heating experiment using an external air-heating method and found that the battery capacity could be increase by 3% with the pre-heating. Ji et al. [149] investigated the convective heating strategy of LIBs using an electrochemical thermal coupled numerical model. The proposed convective heating method can heat the battery both internally and externally. A resistive heater and fan produce an external heating power. An increase in battery temperature of 40 °C can be achieve within 200 s for a heater resistance of 0.6 Ω. Liquid heating is more efficient when compared with air heating. Zhang et al. [150] conducted a series of heating tests on a LIB pack considering using hot liquid fluid and found that the temperature distribution of liquid heating is more uniform compared to that of the other heating methods. The heating efficiency is low for external air or liquid heating method due to the energy loss to the environment through heat conduction. Further, the external heating causes the non-uniform temperature distribution in the LIB pack, which can induce battery degradation. A PCM with high thermal conductivity can significantly reduce the temperature difference in the LIB pack. Ling et al. [151] compared the heating performance of two composites PCM: one with high thermal conductivity (RT44HC/expanded graphite) and the other with low thermal conductivity (RT44HC/fumed silica). The temperature distribution in LIB pack is more uniform using high thermal conductive PCM composite according to the thermal image. Luo et al. [165] conducted the preheating of the battery using the electric-conductive composite PCM (paraffin/expanded graphite). The composite PCM can heat the battery module with the joule heat effect. Results show that an eight-cell battery module can be warmed up with a speed of 13.4 °C/min at a voltage of 3.4 V.

Internal heating with alternating current

The battery heating with alternating current (AC) power source are commonly used internal heating strategies. In AC heating, the battery is heated quickly and uniformly because of the large amount of heat generated inside the battery. Heat is generated by the joule effect of the current passing through the battery, and the current signal in AC heating is a sinusoidal [152–154] or bidirectional current pulse [166,167]. The sinusoidal current pulse is investigated in recent investigations. For AC heating, considerable attention has been paid to the improvement of heating efficiency and the prevention of battery degradation. Zhang et al. [153] conducted experiment test on the battery heating using sinusoidal AC power. Results show that heat generation rate is higher with higher amplitude and lower frequency due to the higher battery polarization. Ruan et al. [154] investigated the influence of alternating frequency on the AC heating performance. Considering the optimal polarization voltage and battery impedance, they discovered an optimum alternating frequency (1377 Hz) for the designed AC heating system. Zhu et al. [152] investigated the influence of current frequency, amplitude, and waveform on the temperature evolution and

Please cite this article as: Jiang ZY et al., Recent progress in lithium-ion battery thermal management for a wide range of temperature and abuse conditions, International Journal of Hydrogen Energy, https://doi.org/10.1016/j.ijhydene.2022.01.008

Table 7 – Summary of recent developments in battery preheating.

S.N.	Heating methods	Heat source	Battery type	Type of study	Temperature rise rate (°C/min)	Ambient temperature (°C)	Variables/Remarks	Year	References
1	External heating	PTC resistance wire	35 Ah $LiMn_2O_4$ power battery	Numerical + Experiment	4.6	−40	Aluminium plate twined by positive temperature coefficient (PTC) resistance wire	2014	Li et al. [146]
2	External heating	Air	Two types of rectangular Li-ion batteries	Numerical	4	−40	Typical rectangular battery heated with four different methods is investigated.	2003	Pesaran et al. [147]
3	External heating	Air	Lithium polymer battery pack	Experiment	0.9	−20	Warm air heating model applied to a battery system is presented.	2012	Song et al. [148]
4	External heating	Air	2.2 Ah cylindrical 18,650 Li-ion battery	Experiment	13.3	−20	Electrical energy consumption, heating time, effect of heating operation, system cost	2013	Ji et al. [149]
5	External heating	Liquid	20 Ah flat cell pack	Experiment	–	−30	Ambient temperature, Reynolds number, flow direction, discharge rate	2002	Zhang et al. [150]
6	External heating	PCM	2.6 Ah 18,650 cylindrical cells	Experiment	–	−10, 5	Battery pack with two composite PCMs with different thermal conductivities is studied.	2018	Ling et al. [151]
7	AC heating	Joule effect	18,650 ($LiMnNiCoO_2$) battery	Experiment	4.96	−24	Frequency, amplitudes, and waveforms of alternating current (AC)	2016	Zhu et al. [152]
8	AC heating	Houle effect	Cylindrical 18,650 cell	Experiment	1.67	−20	Amplitude and frequency of sinusoidal alternating current (AC)	2015	Zhang et al. [153]
9	AC heating	Joule effect	NCM batteries	Numerical + Experiment	3.73	−15.6	Rapid internal heating strategy with the optimal frequency in low-temperature environment is proposed.	2016	Ruan et al. [154]
10	AC heating	Joule effect	30 Ah commercial pouch $LiFePO_4$ cells	Experiment	1.0	−25	Cell degradation, voltage, frequency of AC, internal morphology of battery	2017	Zhu et al. [155]
11	AC heating	Joule effect	18,650 cylindrical lithium-ion battery	Numerical + Experiment	0.75	−20	Layered thermal model based on SAC internal heating strategy is established.	2018	Li et al. [156]
12	AC heating	Joule effect	Laminated three-electrode battery	Experiment	1.875	−20	Multistep, temperature-adaptive and deposition-free AC heating method is proposed.	2016	Ge et al. [157]
13	Self-heating	Ohmic heat	Lithium-ion all-climate battery (ACB) cell	Experiment	60	−20	ACB battery implanted in a nickel foil is established and tested.	2016	Wang et al. [158]

(*continued on next page*)

Table 7 – (continued)

S.N.	Heating methods	Heat source	Battery type	Type of study	Temperature rise rate (°C/min)	Ambient temperature (°C)	Variables/Remarks	Year	References
14	Self-heating	Ohmic heat	Pouch cells	Experiment	96	−20	Two-sheet design of the nickel foil	2016	Zhang et al. [159]
15	Self-heating	Ohmic heat	10 Ah SHLB pouch cell	Experiment	60–120 °C	−20	Battery self–heating method employing SHLB structure is proposed and tested.	2016	Yang et al. [160,161]
16	Self-heating	Wide-line metal film	Prismatic battery	Numerical	–	−20	Numerical model for SHLB structure is established to investigate the temperature uniformity of battery.	2018	Lei et al. [162,163]
17	Self-heating	Pulse self–discharge	2.0 Ah 18,650 lithium-ion battery	Experiment	6.85	−10	Pulse self–discharge strategy with a control circuit is proposed.	2019	Qu et al. [164]

battery performance degradation in AC battery heating. They found that an efficient temperature rise can be achieved with high impedance at low frequencies. Zhu et al. [155] investigated the effect of AC pulse heating method on the battery state of health. They found that cell degradation can be avoided with proper voltage protection limitation when using AC heating method. In addition, the damage on the electrode material induced by continuous discharging or charging could be mitigated by high-frequency changes in the current direction [168]. Li et al. [156] proposed a layered thermal model to simulate a sinusoidal AC heating process. The results showed that the battery capacity is promoted by 45% after heating with the sinusoidal AC current at −20 °C environment temperature. Ge et al. [157] proposed a multistep, temperature-adaptive, and deposition-free AC heating method. The maximum permissible amplitudes of the heating current at different frequencies were determined using equivalent electric circuit model and lithium plating potential.

Battery self-heating method

The aforementioned heating strategies, external heating, and AC heating require an external power source. Heating cannot be initiated when an exterior power source is absent. Therefore, heating strategies using the self–power of a heated LIB have been proposed; such a heating strategy is categorised as a self-heating method. Wang et al. [158] designed a novel self–heating lithium–ion battery structure (SHLB) which can warm up the battery internally from −30 °C to 0 °C within 10 s. The fast heat performance is realized by implanting a nickel foil between electrodes in LIB, which is shown in Fig. 12(a and b). This novel structure provides a practical solution to poor battery performance at low temperatures. Zhang et al. [159] further improved the heating efficiency of SHLB using a two-sheet design of nickel foil. The improved structure consumes 24% less energy than the previous SHLB design with approximating heating performance. Yang et al. [160,161] compared the battery heating of SHLB structure with the external convective heating method. They found that the temperature distribution inside the battery was more uniform for SHLB structure compared to external convective heating method. Lei et al. [162,163] investigated the temperature uniformity in SHLB structure using a numerical model and they found that the temperature uniformity in the battery can be enhanced with lower heating power and smaller thickness. Qu et al. [164] proposed a pulse self–heating strategy which employed the joule heat during the battery discharging. The battery temperature can be increased by 20 °C within 3 min in pulse self-heating test.

Prevention strategies for thermal runaway

Origin of thermal runaway

Benefit from the fast development of novel battery material and fabrication technology, the energy density is significantly increased in recent years [169,170]. However, the thermal safety is not guaranteed by the high energy density material such as NMC 811 [171]. The TR is a critical trepidation for high

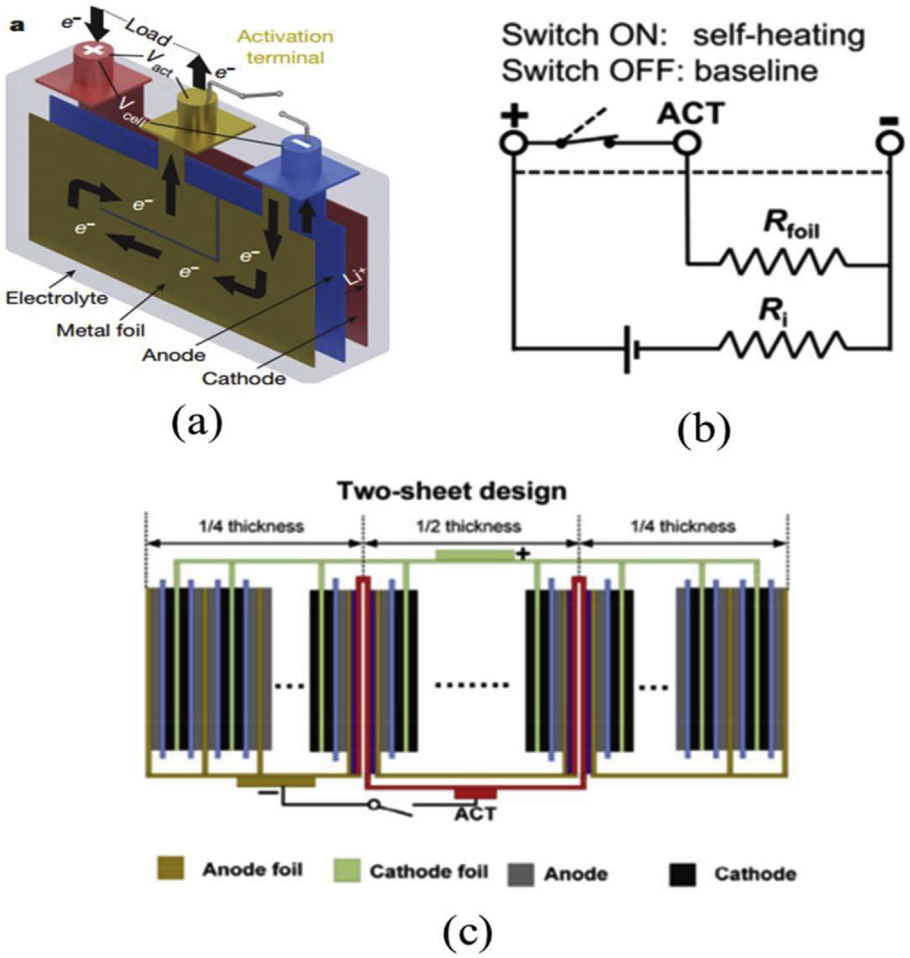

Fig. 12 – Illustration of SHLB structure: (a) SHLB battery structure [159]; (b) SHLB internal circuit structure [159]; (c) two sheet design of SHLB [160].

energy battery. The TR process comprises a battery temperature increase and the decomposition of the battery material [172]. The TR is induced by abuse conditions including mechanical, electrical, and thermal abuse [33,173]. Collisions, crashes, and penetration are typical mechanical abuse condition which can break the separator and induce short circuits of the battery. External short circuit, over-charge, and over-discharge are typical electrical abuse conditions which also induce breakdown of the separator and finally cause an internal short circuit. The electric energy in the battery is released as joule heat in a short time after the internal short circuit releases heat, which initiates thermal abuse. The battery is heated to extreme temperatures and then causes TR under thermal abuse conditions. The failure of a single cell has little influence on the safety of the entire pack. However, the thermal runaway of a single cell can provide enough heat to neighbouring cells within the battery pack to initiate thermal runaway propagation, which can cause the entire battery pack to breakdown and induce severe safety issues.

The features of TR and its propagation in the battery pack have been clarified via experimental measurements and numerical simulations. Feng et al. [174]. Characterises the TR features of a large-format battery using EV-ARC. They studied the penetration-induced TR propagation in a battery module. As shown in Fig. 13(a and b), the penetration-induced TR propagation has a lower onset temperature and a shorter TR triggering time than heating-induced TR in the ARC test [175]. Chen et al. [176] analyzed the fire propagation mechanism in LIBs pack, as shown in Fig. 13 (c). The thermal and fire propagation in LIBs pack will accelerate continuously without proper prevention method (Fig. 13 (d)). In addition to experimental characterization, the analytical and numerical model has been established for TR process. A widely utilised mathematical model has been proposed by Hatchard et al. [177] The temperature variations and material decomposition during TRs are determined using the reaction kinetics of the electrode materials and electrolytes. A well agreement of the temperature curve of oven-exposure testing has been achieved between calculation and experiment. Coman et al. [178] improved the previous mathematical model by introducing the venting process of the electrolyte and jelly roll in the calculation. They found that ejection of the electrolyte and jelly roll contents induced the heat dissipation during TRs. The failure of a single cell can generate sufficient heat to initiate the TR in surrounding cells. This process is termed as TR propagation which is the greatest danger of TR in LIB pack.

Please cite this article as: Jiang ZY et al., Recent progress in lithium-ion battery thermal management for a wide range of temperature and abuse conditions, International Journal of Hydrogen Energy, https://doi.org/10.1016/j.ijhydene.2022.01.008

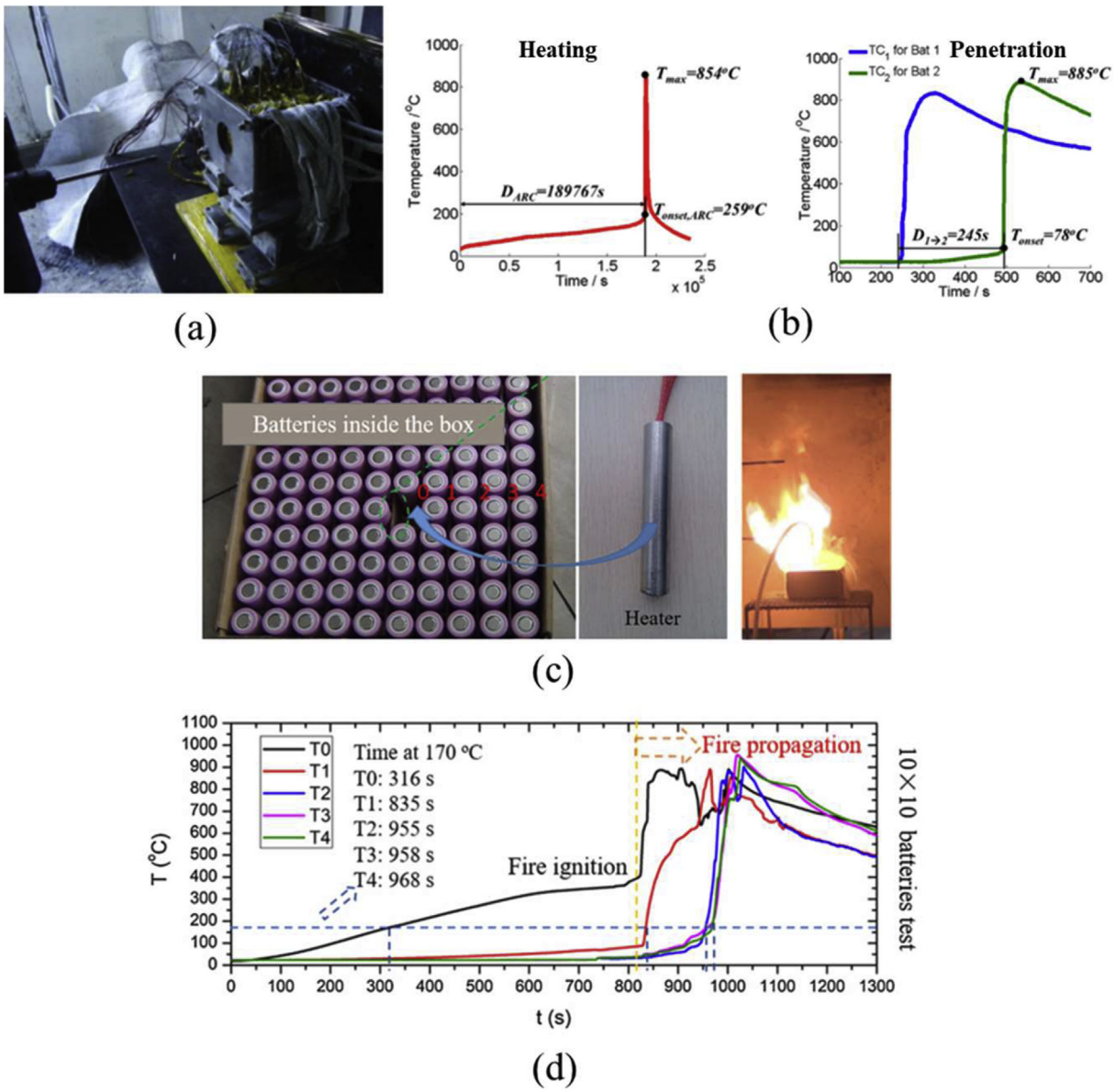

Fig. 13 – TR propagation in battery pack: (a) penetration test of battery module [175]; (b) comparison of TR onset induced by heating and penetration [175]; (c) fire propagation test in battery pack [176]; (d) temperature variation in battery pack during TR propagation [176].

Further, TR propagation models are established. Yeowe et al. [179] investigated the TR propagation process in a LIB module composed of three pouch cells using 3D numerical model. They found that a minimum temperature of 165 °C in central cell is required to trigger the TR in the module. Yang et al. [180] investigated the TR propagation in LIB pack composed of ten large-format cells. A 3D model is built for simulating thermal, mechanical, and electrical abuse during TR. Feng et al. [181] discussed the mechanisms for the delay in TR propagation using a 3D TR model. They stated that the 3D model provided more information on the temperature distribution. The 3D modelling of TR propagation consumes much time and computation sources. Therefore, Spotnitz et al. [182] proposed a lumped thermal model to simulate the TR propagation in LIB pack composed of 18,650 cells. They stressed the importance of contact between cells during the TR process. Smith et al. [183] further introduced the electric model in the lumped TR propagation model and both the electric and thermal responds of the battery can be obtained during TR. The numerical results were assessed using external short-circuit tests. In addition to the 18,650 cells, Feng et al. [184] investigated the TR propagation in large-format LIBs using lumped thermal model. Their study provides the proper parameters that help to postpone or prevent TR propagation in battery pack structures. The numerical simulation using lumped thermal model has been proved to be a powerful tool for investigating TR propagation in LiB pack, but the key thermal properties of battery assemblies should be accurately characterised to acquire a reasonable modelling result.

Please cite this article as: Jiang ZY et al., Recent progress in lithium-ion battery thermal management for a wide range of temperature and abuse conditions, International Journal of Hydrogen Energy, https://doi.org/10.1016/j.ijhydene.2022.01.008

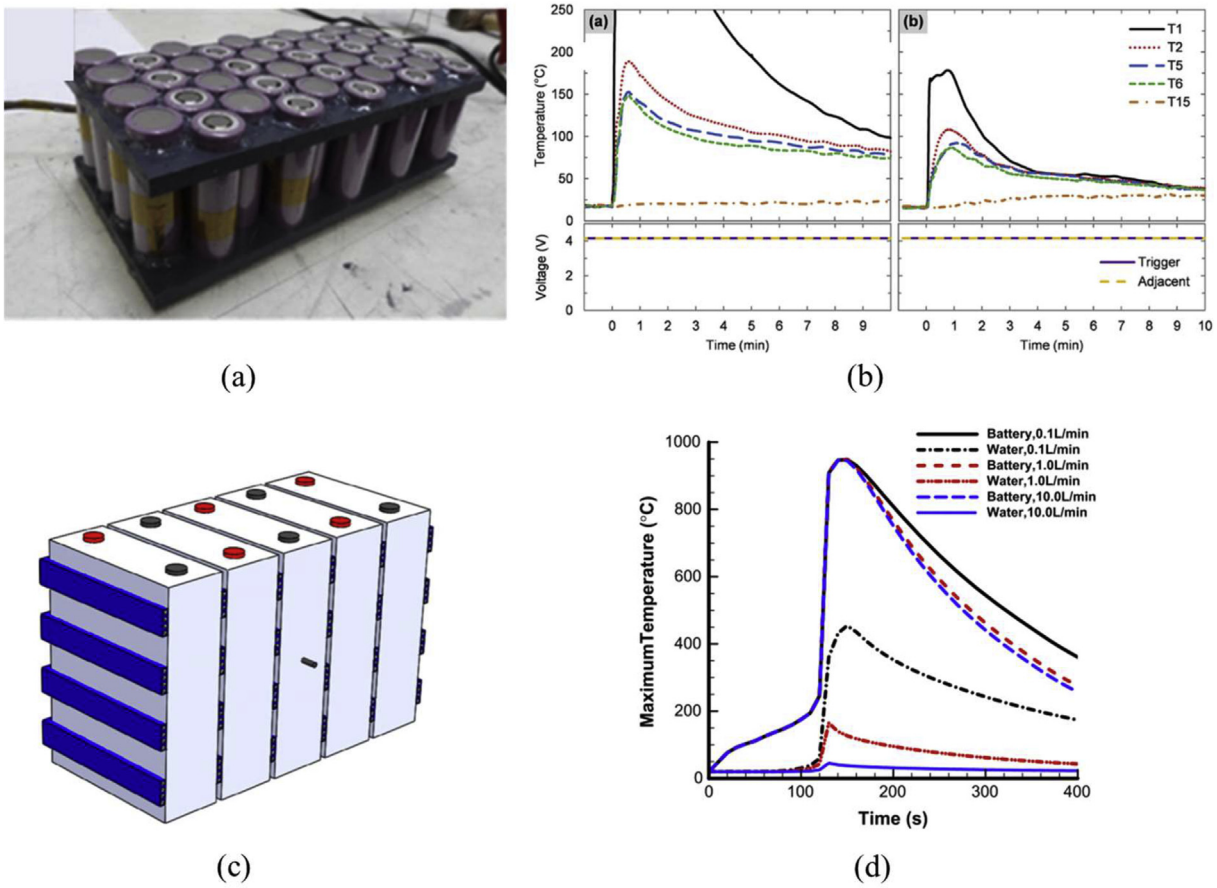

Fig. 14 – TR prevention and mitigation structure: (a) TR prevention with phase change composite; (b) comparison of temperature profile without and with phase change composite [195]; (c) TR mitigation using mini-channel [196]; (d) temperature profiles with the cooling of mini-channel [196].

Prevention of thermal runaway from material perspective

The modifications to the cathode, anode, separator, and electrolyte were conducted to build a robust battery chemical structure. The primary objective of inventing new battery component materials and material modification is preventing the formation of chain reactions during TR propagation. Coating the cathode material is the most common approach for improving the thermal stability of cathodes. Phosphates [185,186], fluorides [187] and solid oxides [188,189] are favoured coating materials for cathodes. Cho [185] investigated the overcharge behaviour of an AlPO4 coated LiCoO2 cathode. The oven test experiment suggested that the $AlPO_4$ coating layer stabilised the cathode material. Sun et al. [187] used amorphous AlF_3 as coating material for improving the performance of a NMC cathode. The cyclic performance and rate capability of AlF_3-coated electrode are improved under the high cut-off voltage of 4.5 V. Li et al. [188] investigated the $FePO_4$-coated $LiCoO_2$ cathode under a high charge cut-off voltage. The results indicated that the improved $LiCoO_2$ cathode shows better anti-overcharge and thermal safety performance. Hu et al. [189] investigated ZrO_2-coated spherical $LiNi_{1/3}Co_{1/3}Mn_{1/3}O_2$ cathodes. In their study, an improved rate capability and cycling stability was achieved for the ZrO_2-coated $LiNi_{1/3}Co_{1/3}Mn_{1/3}O_2$ material under a high cut-off voltage of 4.5 V. Yun et al. [190] compared the electrochemical performance of pristine and ZrFx-coated NMC cathode materials. The better rate capability and cyclic performance are achieved for the coated cathode electrodes. Kobayashi et al. [191] prepared an Al_2O_3-coated $Li_{1.2}Mn_{0.55}Ni_{0.16}Co_{0.09}O_2$ cathode using a mechanical reaction. The results show that the mechanochemical Al_2O_3 coating process can improve the high temperature cyclic performance of electrode. Cho et al. [192] investigated the cycling performance of SiO_2-coated Ni rich $LiNi_{0.6}Co_{0.2}Mn_{0.2}O_2$ cathode material. The experimental results show that a better cycling performance is obtained with the coated cathode at a high temperature of 60 °C. They further used manganese orthophosphate ($Mn_3(PO_4)_2$) as a new coating material [193]. The coated electrode exhibited an improved rate capability at a high current drain, and the cycle performance was enhanced at a high temperature of 60 °C. Ji et al. [194] proposed a novel temperature-responsive cathode by coating an ultrathin layer of poly (3-octylthiophene). The PTC behaviour of coating material can switch off the cell reaction at high temperature range of 90–100 °C, which could stop the internal short in TR.

Prevention of thermal runaway from thermal management perspective

The prevention of TR and its propagation is a critical issue after determining TR behaviour. As shown in Fig. 14 (a), Wilke et al. [195] investigated the prevention effect of a phase change composite (PCC) on the TR propagation induced by the nail penetration. The results show LIB pack with PCC can completely avoid the TR propagation due to the heat absorption of PCM, as indicated in Fig. 14 (b). Xu et al. [196] designed a mini-channel cooling system for the mitigation of TR, as shown in Fig. 14 (c). They found that mini-channel cooling can sufficiently mitigate the heat transfer between adjacent cells during TR propagation, as shown in Fig. 14 (d). Li et al. [197] proposed a TR mitigation structure using aluminium plates assembled into a battery pack. They found that thermal mass of cooling plate and contact resistance between cell and cooling plate are key parameters that prevent thermal runaway. Mohammadian et al. [198] investigated the effects of using microchannels on the prevention of battery TR. The lattice Boltzmann method simulation was conducted based on the pore-scale porous electrode. Further, the mini-channel could lead the gases out of the electrode, which mitigate the TR occurrence.

Summary and prospect

Li-ion batteries is becoming the primary power source for EVs in recent years. Although extensive efforts have been invested in researching battery materials, battery thermal management remains a critical issue that hinders the development of battery applications. In this paper, recent progress in the thermal management of LiBs was reviewed. The heat generation mechanism was characterised using experimental and mathematical models. Different battery cooling methods were comprehensively discussed. For air cooling, most research interest focused on the optimisation of air-cooling structures, and the objective of recent investigations was to improve the heat transfer efficiency by introducing new air flow paths or setting locations of the inlet and outlet. The mini-channel cold plate has become a research interest in recent years, with the selection of working fluids and channel geometry optimisation being frequently discussed. The thermal conductivity enhancement of PCMs continues to remain a hot topic in PCM cooling research. Considerable attention has been paid to the long-term cycling performance of PCMs, and the utilisation of heat pipes is treated as a highly thermally conductive medium that can transfer heat from the battery to the heat sink. The heat pipe is always coupled with other cooling methods in real applications. A combination of different cooling methods is an optimal solution for battery thermal management, and investigations on the coupling of PCM cooling and forced air or liquid cooling increase because of the excellent balance of cooling performance and cost. Battery-heating techniques have been comparatively neglected because of the extensive attention afforded to battery cooling. AC heating is the preferred heating method because of its high heat generation efficiency and low battery cycling life. The investigations focused on exploring the optimal alternating frequency and allowable safe voltage range. An efficient self-heating method—self–heating lithium–ion battery structure (SHLB)—was proposed to enable a fast and safe self-heating process. The battery TR and its propagation were investigated through experiments and numerical simulations, and the TR heat generation and propagation features were determined. The PCM, mini-channel, and metallic plates were employed to prevent TR. Further, it was found that TR is difficult to terminate in a single cell, and the propagation process can be prevented using the present thermal management methods.

Lithium ion batteries are developing towards high energy density and high-power density. At the same time, the heat generation power increases with the increase of battery volume, and the uneven surface temperature of single battery becomes more significant. Three important issues are still need investigation in the near future: First, the existing cooling methods need to be refined to perform more sufficient cooling capability with less energy consumption and equipment mass and volume. Specifically, the Liquid-based system designs are expected to consume less energy according to the objective functions of pressure drop, temperature drop, and uniformity. Reducing the additional volume and quality is an important issue for PCM-based BTMS used in a conventional environment. In the hybrid PCM-based BTMS coupled with a liquid cooling system, the improvement of the structure of the cooling system and performance of cooling fluid will be the focus of studies for improving the thermal management efficiency and control strategy of system. For battery heating methods, the heating strategies for battery pack level needs further investigation to overcome the cell temperature inhomogeneity in a pack. The development of model-based heating control strategies in BTMS are also critical for optimal battery heating performance. Second, a coupling system that can cover battery cooling and heating is still unavailable, the thermal management for wide temperature range is urgent. Novel methods such as using composite PCM and adsorption heating effect need to be further explored to realise the passive wide temperature control. Third, the TR prevention and mitigation methods are still insufficient. The liquid cooling, PCM cooling and spray cooling methods are promising strategies for heat dissipation of TR. The TR propagation characteristic in battery pack has not been well understood. Mechanism explore on the combustible gas composition, hot gas flow and fire propagation should be further conducted. Moreover, due to the fast heat release of TR process, cooling and fire control system that can rapid respond to TR needs development.

Declaration of competing interest

The authors declare that they have no known competing financial interests or personal relationships that could have appeared to influence the work reported in this paper.

Acknowledgment

This work was financially supported by the National Science Foundation for Distinguished Young Scholars (No. 52025065), the Basic Science Center Program for Ordered Energy

Conversion of the National Natural Science Foundation of China (No.51888103), the National Natural Science Foundation of China (No. 52106111), and the Fundamental Research Funds for the Central Universities (No. xzy012021036).

REFERENCES

[1] Zou J, Han N, Yan J, Feng Q, Wang Y, Zhao Z, et al. Electrochemical compression technologies for high-pressure hydrogen: current status, challenges and perspective. Electrochem Energy R 2020;3:690–729.
[2] Koontz DE, Feder DO, Babusci LD, Luer HJ. Lead-acid battery: reserve batteries for bell system use: design of the new cell. Bell System Technical J 1970;49:1253–78.
[3] Huang B, Pan Z, Su X, An L. Recycling of lithium-ion batteries: recent advances and perspectives. J Power Sources 2018;399:274–86.
[4] Jamesh M-I. Recent advances on flexible electrodes for Na-ion batteries and Li–S batteries. J Energy Chem 2019;32:15–44.
[5] Ghimire PC, Bhattarai A, Schweiss R, Scherer GG, Wai N, Yan Q. A comprehensive study of electrode compression effects in all vanadium redox flow batteries including locally resolved measurements. Appl Energy 2018;230:974–82.
[6] Baumann L, Boggasch E. Experimental assessment of hydrogen systems and vanadium-redox-flow-batteries for increasing the self-consumption of photovoltaic energy in buildings. Int J Hydrogen Energy 2016;41:740–51.
[7] Yang S, Zhang Z, Cao R, Wang M, Cheng H, Zhang L, et al. Implementation for a cloud battery management system based on the CHAIN framework. Energy and AI 2021:5.
[8] Yang S, He R, Zhang Z, Cao Y, Gao X, Liu X. CHAIN: cyber hierarchy and interactional network enabling digital solution for battery full-lifespan management. Matter 2020;3:27–41.
[9] Ouyang M. A dynamic capacity degradation model and its applications considering varying load for a large format Li-ion battery. Appl Energy 2016;165:48–59.
[10] Waldmann T, Wilka M, Kasper M, Fleischhammer M, Wohlfahrt-Mehrens M. Temperature dependent ageing mechanisms in Lithium-ion batteries – a Post-Mortem study. J Power Sources 2014;262:129–35.
[11] Feng X, Mou F, He X, Ouyang M, Lu L, Hao W, et al. Thermal runaway features of large format prismatic lithium ion battery using extended volume accelerating rate calorimetry. J Power Sources 2014;255:294–301.
[12] Huang P, Ping P, Ke L, Chen H, Wang Q, Wen J, et al. Experimental and modeling analysis of thermal runaway propagation over the large format energy storage battery module with Li 4 Ti 5 O 12 anode. Appl Energy 2016;183:659–73.
[13] Wang Q, Ping P, Zhao X, Chu G, Sun J, Chen C. Thermal runaway caused fire and explosion of lithium ion battery. J Power Sources 2012;208:210–24.
[14] Maleki H, Howard JN. Internal short circuit in Li-ion cells. J Power Sources 2009;191:568–74.
[15] Lai WJ, Ali MY, Pan J. Mechanical behavior of representative volume elements of lithium-ion battery modules under various loading conditions. J Power Sources 2014;248:789–808.
[16] Greve L, Fehrenbach C. Mechanical testing and macro-mechanical finite element simulation of the deformation, fracture, and short circuit initiation of cylindrical Lithium ion battery cells. J Power Sources 2012;214:377–85.
[17] Smith K, Kim G-H, Darcy E, Pesaran A. Thermal/electrical modeling for abuse-tolerant design of lithium ion modules. Int J Energy Res 2010;34:204–15.
[18] Zheng Y, Han X, Lu L, Li J, Ouyang M. Lithium ion battery pack power fade fault identification based on Shannon entropy in electric vehicles. J Power Sources 2013;223:136–46.
[19] Kitoh K, Nemoto H. 100 Wh Large size Li-ion batteries and safety tests. J Power Sources 1999;81–82:887–90.
[20] Spotnitz R, Franklin J. Abuse behavior of high-power, lithium-ion cells. J Power Sources 2003;113:81–100.
[21] Ouyang M, Ren D, Lu L, Li J, Feng X, Han X, et al. Overcharge-induced capacity fading analysis for large format lithium-ion batteries with LiyNi1/3Co1/3Mn1/3O2+LiyMn2O4 composite cathode. J Power Sources 2015;279:626–35.
[22] Zhang L, Ma Y, Cheng X, Du C, Guan T, Cui Y, et al. Capacity fading mechanism during long-term cycling of over-discharged LiCoO2/mesocarbon microbeads battery. J Power Sources 2015;293:1006–15.
[23] Zhang SS, Xu K, Jow TR. The low temperature performance of Li-ion batteries. J Power Sources 2003;115:137–40.
[24] Shiao HC, Chua D, Lin HP, Slane S, Salomon M. Low temperature electrolytes for Li-ion PVDF cells. J Power Sources 2000;87:167–73.
[25] Zhang SS, Xu K, Jow TR. Charge and discharge characteristics of a commercial LiCoO 2 -based 18650 Li-ion battery. J Power Sources 2006;160:1403–9.
[26] Huang CK, Sakamoto J, Wolfenstine J, Surampudi S. The limits of low-temperature performance of Li-ion cells. J Electrochem Soc 2000;147:2893–6.
[27] Tippmann Simon, Walper Daniel, Balboa Luis, et al. Low-temperature charging of lithium-ion cells part I: electrochemical modeling and experimental investigation of degradation behavior. J Power Sources 2014;252:305–16.
[28] Li Y, Feng X, Ren D, Ouyang M, Lu L, Han X. Thermal runaway triggered by plated lithium on the anode after fast charging. ACS Appl Mater Interfaces 2019;11:46839–50.
[29] Li Y, Gao X, Feng X, Ren D, Li Y, Hou J, et al. Battery eruption triggered by plated lithium on an anode during thermal runaway after fast charging. Energy 2022:239.
[30] Liu H, Wei Z, He W, Zhao J. Thermal issues about Li-ion batteries and recent progress in battery thermal management systems: a review. Energy Convers Manag 2017;150:304–30.
[31] Xia G, Cao L, Bi G. A review on battery thermal management in electric vehicle application. J Power Sources 2017;367:90–105.
[32] Deng Y, Feng C, E J, Zhu H, Chen J, Wen M, et al. Effects of different coolants and cooling strategies on the cooling performance of the power lithium ion battery system: a review. Appl Therm Eng 2018;142:10–29.
[33] Feng X, Ouyang M, Liu X, Lu L, Xia Y, He X. Thermal runaway mechanism of lithium ion battery for electric vehicles: a review. Energy Storage Mater 2018;10:246–67.
[34] Chen J, Kang S, E J, Huang Z, Wei K, Zhang B, et al. Effects of different phase change material thermal management strategies on the cooling performance of the power lithium ion batteries: a review. J Power Sources 2019;442:227228.
[35] Peng X, Chen S, Garg A, Bao N, Panda B. A review of the estimation and heating methods for lithium-ion batteries pack at the cold environment. Energy Sci Eng 2019;7:645–62.
[36] Wu W, Wang S, Wu W, Chen K, Hong S, Lai Y. A critical review of battery thermal performance and liquid based battery thermal management. Energy Convers Manag 2019;182:262–81.
[37] Akinlabi AAH, Solyali D. Configuration, design, and optimization of air-cooled battery thermal management

Please cite this article as: Jiang ZY et al., Recent progress in lithium-ion battery thermal management for a wide range of temperature and abuse conditions, International Journal of Hydrogen Energy, https://doi.org/10.1016/j.ijhydene.2022.01.008

system for electric vehicles: a review. Renew Sustain Energy Rev 2020;125:109815.
[38] Aswin Karthik C, Kalita P, Cui X, Peng X. Thermal management for prevention of failures of lithium ion battery packs in electric vehicles: a review and critical future aspects. Energy Storage 2020;2.
[39] Duan J, Tang X, Dai H, Yang Y, Wu W, Wei X, et al. Building safe lithium-ion batteries for electric vehicles: a review. Electrochem Energy R 2020;3:1–42.
[40] Tete PR, Gupta MM, Joshi SS. Developments in battery thermal management systems for electric vehicles: a technical review. J Storage Mater 2021;35:102255.
[41] Bandhauer TM, Garimella S, Fuller TF. A critical review of thermal issues in lithium-ion batteries. J Electrochem Soc 2011;158:R1.
[42] Bernard Ep D, Newman J. A general energy balance for battery systems. J Electrochem Soc 1985;132:5–12.
[43] Liu G, Ouyang M, Lu L, Li J, Han X. Analysis of the heat generation of lithium-ion battery during charging and discharging considering different influencing factors. J Therm Anal Calorim 2014;116:1001–10.
[44] Tong W, Somasundaram K, Birgersson E, Mujumdar AS, Yap C. Thermo-electrochemical model for forced convection air cooling of a lithium-ion battery module. Appl Therm Eng 2016;99:672–82.
[45] Strange C, dos Reis G. Prediction of future capacity and internal resistance of Li-ion cells from one cycle of input data. Energy and AI 2021;5:100097.
[46] Carnovale A, Li X. A modeling and experimental study of capacity fade for lithium-ion batteries. Energy and AI 2020;2:100032.
[47] Thomas KE, Newman J. Thermal modeling of porous insertion electrodes. J Electrochem Soc 2003;150:A176.
[48] Lai Y, Du S, Ai L, Ai L, Cheng Y, Tang Y, et al. Insight into heat generation of lithium ion batteries based on the electrochemical-thermal model at high discharge rates. Int J Hydrogen Energy 2015;40:13039–49.
[49] Onda K, Ohshima T, Nakayama M, Fukuda K, Araki T. Thermal behavior of small lithium-ion battery during rapid charge and discharge cycles. J Power Sources 2006;158:535–42.
[50] Claude F, Becherif M, Ramadan HS. Experimental validation for Li-ion battery modeling using Extended Kalman Filters. Int J Hydrogen Energy 2017;42:25509–17.
[51] Nazari A, Farhad S. Heat generation in lithium-ion batteries with different nominal capacities and chemistries. Appl Therm Eng 2017;125:1501–17.
[52] Bandhauer TM, Garimella S, Fuller TF. Temperature-dependent electrochemical heat generation in a commercial lithium-ion battery. J Power Sources 2014;247:618–28.
[53] Lin C, Xu S, Liu J. Measurement of heat generation in a 40 Ah LiFePO4 prismatic battery using accelerating rate calorimetry. Int J Hydrogen Energy 2018;43:8375–84.
[54] Ishikawa H, Mendoza O, Sone Y, Umeda M. Study of thermal deterioration of lithium-ion secondary cell using an accelerated rate calorimeter (ARC) and AC impedance method. J Power Sources 2012;198:236–42.
[55] Jhu CY, Wang YW, Wen CY, Shu CM. Thermal runaway potential of LiCoO2 and Li(Ni1/3Co1/3Mn1/3)O2 batteries determined with adiabatic calorimetry methodology. Appl Energy 2012;100:127–31.
[56] Lu W, Belharouak I, Park SH, Sun YK, Amine K. Isothermal calorimetry investigation of Li1+xMn2−yAlzO4 spinel. Electrochim Acta 2007;52:5837–42.
[57] Millet LBM, Raab P. Isothermal calorimeter heat measurements of a 20Ah lithium iron phosphate battery cell. Twelfth Int Conf Ecolog Vehicles & Ren Energies IEEE 2017:1–7.
[58] Freyer MW, Lewis EA. Isothermal Titration Calorimetry: experimental design, data analysis, and probing macromolecule/ligand binding and kinetic interactions. Methods in Cell Biology: Academic Press; 2008. p. 79–113.
[59] Heubner C, Schneider M, Lämmel C, Michaelis A. Local heat generation in a single stack lithium ion battery cell. Electrochim Acta 2015;186:404–12.
[60] Vishwakarma V, Waghela C, Wei Z, Prasher R, Nagpure SC, Li J, et al. Heat transfer enhancement in a lithium-ion cell through improved material-level thermal transport. J Power Sources 2015;300:123–31.
[61] Drake SJ, Wetz DA, Ostanek JK, Miller SP, Heinzel JM, Jain A. Measurement of anisotropic thermophysical properties of cylindrical Li-ion cells. J Power Sources 2014;252:298–304.
[62] Nanda J, Martha SK, Porter WD, Wang H, Dudney NJ, Radin MD, et al. Thermophysical properties of LiFePO4 cathodes with carbonized pitch coatings and organic binders: experiments and first-principles modeling. J Power Sources 2014;251:8–13.
[63] Cho J, Losego MD, Zhang HG, Kim H, Zuo J, Petrov I, et al. Electrochemically tunable thermal conductivity of lithium cobalt oxide. Nat Commun 2014;5:4035.
[64] Vishwakarma V, Jain A. Measurement of in-plane thermal conductivity and heat capacity of separator in Li-ion cells using a transient DC heating method. J Power Sources 2014;272:378–85.
[65] Gaitonde A, Nimmagadda A, Marconnet A. Measurement of interfacial thermal conductance in Lithium ion batteries. J Power Sources 2017;343:431–6.
[66] Shih N-C, Lin C-L, Chang C-C, Wang D-Y. Experimental tests of an air-cooling hydrogen fuel cell hybrid electric scooter. Int J Hydrogen Energy 2013;38:11144–8.
[67] Chen K, Chen Y, Li Z, Yuan F, Wang S. Design of the cell spacings of battery pack in parallel air-cooled battery thermal management system. Int J Heat Mass Tran 2018;127:393–401.
[68] Chen K, Song M, Wei W, Wang S. Structure optimization of parallel air-cooled battery thermal management system with U-type flow for cooling efficiency improvement. Energy 2018;145:603–13.
[69] Kirad K, Chaudhari M. Design of cell spacing in lithium-ion battery module for improvement in cooling performance of the battery thermal management system. J Power Sources 2021;481:229016.
[70] Fan Y, Bao Y, Ling C, Chu Y, Tan X, Yang S. Experimental study on the thermal management performance of air cooling for high energy density cylindrical lithium-ion batteries. Appl Therm Eng 2019;155:96–109.
[71] Lu Z, Yu X, Wei L, Qiu Y, Zhang L, Meng X, et al. Parametric study of forced air cooling strategy for lithium-ion battery pack with staggered arrangement. Appl Therm Eng 2018;136:28–40.
[72] Wang T, Tseng KJ, Zhao J, Wei Z. Thermal investigation of lithium-ion battery module with different cell arrangement structures and forced air-cooling strategies. Appl Energy 2014;134:229–38.
[73] Peng X, Ma C, Garg A, Bao N, Liao X. Thermal performance investigation of an air-cooled lithium-ion battery pack considering the inconsistency of battery cells. Appl Therm Eng 2019;153:596–603.
[74] Ji C, Wang B, Wang S, Pan S, Wang D, Qi P, et al. Optimization on uniformity of lithium-ion cylindrical battery module by different arrangement strategy. Appl Therm Eng 2019;157:113683.

Please cite this article as: Jiang ZY et al., Recent progress in lithium-ion battery thermal management for a wide range of temperature and abuse conditions, International Journal of Hydrogen Energy, https://doi.org/10.1016/j.ijhydene.2022.01.008

[75] Li W, Xiao M, Peng X, Garg A, Gao L. A surrogate thermal modeling and parametric optimization of battery pack with air cooling for EVs. Appl Therm Eng 2019;147:90–100.
[76] Zhou H, Zhou F, Xu L, Kong J, Qingxin Yang. Thermal performance of cylindrical Lithium-ion battery thermal management system based on air distribution pipe. Int J Heat Mass Tran 2019;131:984–98.
[77] E J, Yue M, Chen J, Zhu H, Deng Y, Zhu Y, et al. Effects of the different air cooling strategies on cooling performance of a lithium-ion battery module with baffle. Appl Therm Eng 2018;144:231–41.
[78] Xie J, Xie Y, Yuan C. Numerical study of heat transfer enhancement using vortex generator for thermal management of lithium ion battery. Int J Heat Mass Tran 2019;129:1184–93.
[79] Yu K, Yang X, Cheng Y, Li C. Thermal analysis and two-directional air flow thermal management for lithium-ion battery pack. J Power Sources 2014;270:193–200.
[80] Li X, He F, Zhang G, Huang Q, Zhou D. Experiment and simulation for pouch battery with silica cooling plates and copper mesh based air cooling thermal management system. Appl Therm Eng 2019;146:866–80.
[81] Zhao R, Liu J, Gu J, Zhai L, Ma F. Experimental study of a direct evaporative cooling approach for Li-ion battery thermal management. Int J Energy Res 2020;44:6660–73.
[82] Lai Y, Wu W, Chen K, Wang S, Xin C. A compact and lightweight liquid-cooled thermal management solution for cylindrical lithium-ion power battery pack. Int J Heat Mass Tran 2019;144:118581.
[83] Shen J, Wang Y, Yu G, Li H. Thermal management of prismatic lithium-ion battery with minichannel cold plate. J Energy Eng 2020;146:04019033.
[84] Madani SS, Schaltz E, Kær SK. Thermal analysis of cold plate with different configurations for thermal management of a lithium-ion battery. Batteries 2020;6:17.
[85] Lv Y, Zhou D, Yang X, Liu X, Li X, Zhang G. Experimental investigation on a novel liquid-cooling strategy by coupling with graphene-modified silica gel for the thermal management of cylindrical battery. Appl Therm Eng 2019;159:113885.
[86] Menale C, D'Annibale F, Mazzarotta B, Bubbico R. Thermal management of lithium-ion batteries: an experimental investigation. Energy 2019;182:57–71.
[87] Liu Z, Wang H, Yang C, Zhao J. Simulation study of lithium-ion battery thermal management system based on a variable flow velocity method with liquid metal. Appl Therm Eng 2020;179:115578.
[88] Zhou H, Zhou F, Zhang Q, Wang Q, Song Z. Thermal management of cylindrical lithium-ion battery based on a liquid cooling method with half-helical duct. Appl Therm Eng 2019;162:114257.
[89] Rao Z, Qian Z, Kuang Y, Li Y. Thermal performance of liquid cooling based thermal management system for cylindrical lithium-ion battery module with variable contact surface. Appl Therm Eng 2017;123:1514–22.
[90] Shang Z, Qi H, Liu X, Ouyang C, Wang Y. Structural optimization of lithium-ion battery for improving thermal performance based on a liquid cooling system. Int J Heat Mass Tran 2019;130:33–41.
[91] Panchal S, Khasow R, Dincer I, Agelin-Chaab M, Fraser R, Fowler M. Thermal design and simulation of mini-channel cold plate for water cooled large sized prismatic lithium-ion battery. Appl Therm Eng 2017;122:80–90.
[92] An Z, Jia L, Li X, Ding Y. Experimental investigation on lithium-ion battery thermal management based on flow boiling in mini-channel. Appl Therm Eng 2017;117:534–43.
[93] Yates M, Akrami M, Javadi AA. Analysing the performance of liquid cooling designs in cylindrical lithium-ion batteries. J Storage Mater 2019:100913.
[94] Deng T, Zhang G, Ran Y, Liu P. Thermal performance of lithium ion battery pack by using cold plate. Appl Therm Eng 2019;160:114088.
[95] Du J, Sun Y, Huang Y, Wu X. Analysis of influencing factors of thermal management system for LiFePO4 lithium battery under high power charging. World Electric Vehicle Journal 2020;11:44.
[96] Xu X, Li W, Xu B, Qin J. Numerical study on a water cooling system for prismatic LiFePO4 batteries at abused operating conditions. Appl Energy 2019;250:404–12.
[97] Li Y, Zhou Z, Wu W-T. Three-dimensional thermal modeling of Li-ion battery cell and 50 V Li-ion battery pack cooled by mini-channel cold plate. Appl Therm Eng 2019;147:829–40.
[98] Yang W, Zhou F, Zhou H, Wang Q, Kong J. Thermal performance of cylindrical lithium-ion battery thermal management system integrated with mini-channel liquid cooling and air cooling. Appl Therm Eng 2020;175:115331.
[99] Huang Y, Mei P, Lu Y, Huang R, Yu X, Chen Z, et al. A novel approach for Lithium-ion battery thermal management with streamline shape mini channel cooling plates. Appl Therm Eng 2019;157:113623.
[100] Chen S, Peng X, Bao N, Garg A. A comprehensive analysis and optimization process for an integrated liquid cooling plate for a prismatic lithium-ion battery module. Appl Therm Eng 2019;156:324–39.
[101] Du X, Qian Z, Chen Z, Rao Z. Experimental investigation on mini-channel cooling-based thermal management for Li-ion battery module under different cooling schemes. Int J Energy Res 2018;42:2781–8.
[102] Li X, Huang Q, Deng J, Zhang G, Zhong Z, He F. Evaluation of lithium battery thermal management using sealant made of boron nitride and silicone. J Power Sources 2020;451:227820.
[103] Kizilel R, Lateef A, Sabbah R, Farid MM, Selman JR, Al-Hallaj S. Passive control of temperature excursion and uniformity in high-energy Li-ion battery packs at high current and ambient temperature. J Power Sources 2008;183:370–5.
[104] Khateeb SA, Amiruddin S, Farid M, Selman JR, Al-Hallaj S. Thermal management of Li-ion battery with phase change material for electric scooters: experimental validation. J Power Sources 2005;142:345–53.
[105] Rao Z, Wang S, Zhang G. Simulation and experiment of thermal energy management with phase change material for ageing LiFePO4 power battery. Energy Convers Manag 2011;52:3408–14.
[106] Liu W, Jia Z, Luo Y, Xie W, Deng T. Experimental investigation on thermal management of cylindrical Li-ion battery pack based on vapor chamber combined with fin structure. Appl Therm Eng 2019;162:114272.
[107] Ren Y, Yu Z, Song G. Thermal management of a Li-ion battery pack employing water evaporation. J Power Sources 2017;360:166–71.
[108] Saw LH, Poon HM, Thiam HS, Cai Z, Chong WT, Pambudi NA, et al. Novel thermal management system using mist cooling for lithium-ion battery packs. Appl Energy 2018;223:146–58.
[109] Farid MM, Khudhair AM, Razack SAK, Al-Hallaj S. A review on phase change energy storage: materials and applications. Energy Convers Manag 2004;45:1597–615.
[110] Azizi Y, Sadrameli SM. Thermal management of a LiFePO4 battery pack at high temperature environment using a

Please cite this article as: Jiang ZY et al., Recent progress in lithium-ion battery thermal management for a wide range of temperature and abuse conditions, International Journal of Hydrogen Energy, https://doi.org/10.1016/j.ijhydene.2022.01.008

composite of phase change materials and aluminum wire mesh plates. Energy Convers Manag 2016;128:294–302.
[111] Li WQ, Qu ZG, He YL, Tao YB. Experimental study of a passive thermal management system for high-powered lithium ion batteries using porous metal foam saturated with phase change materials. J Power Sources 2014;255:9–15.
[112] Qu ZG, Li WQ, Tao WQ. Numerical model of the passive thermal management system for high-power lithium ion battery by using porous metal foam saturated with phase change material. Int J Hydrogen Energy 2014;39:3904–13.
[113] Zhu WH, Yang H, Webb K, Barron T, Dimick P, Tatarchuk BJ. A novel cooling structure with a matrix block of microfibrous media/phase change materials for heat transfer enhancement in high power Li-ion battery packs. J Clean Prod 2019;210:542–51.
[114] Li WQ, Qu ZG, He YL, Tao WQ. Experimental and numerical studies on melting phase change heat transfer in open-cell metallic foams filled with paraffin. Appl Therm Eng 2012;37:1–9.
[115] Samimi F, Babapoor A, Azizi M, Karimi G. Thermal management analysis of a Li-ion battery cell using phase change material loaded with carbon fibers. Energy 2016;96:355–71.
[116] Babapoor A, Azizi M, Karimi G. Thermal management of a Li-ion battery using carbon fiber-PCM composites. Appl Therm Eng 2015;82:281–90.
[117] Goli P, Legedza S, Dhar A, Salgado R, Renteria J, Balandin AA. Graphene-enhanced hybrid phase change materials for thermal management of Li-ion batteries. J Power Sources 2014;248:37–43.
[118] Huang Y-H, Cheng W-L, Zhao R. Thermal management of Li-ion battery pack with the application of flexible form-stable composite phase change materials. Energy Convers Manag 2019;182:9–20.
[119] Luo X, Guo Q, Li X, Tao Z, Lei S, Liu J, et al. Experimental investigation on a novel phase change material composites coupled with graphite film used for thermal management of lithium-ion batteries. Renew Energy 2020;145:2046–55.
[120] Wang W, Zhang X, Xin C, Rao Z. An experimental study on thermal management of lithium ion battery packs using an improved passive method. Appl Therm Eng 2018;134:163–70.
[121] Koyama R, Arai Y, Yamauchi Y, Takeya S, Endo F, Hotta A, et al. Thermophysical properties of trimethylolethane (TME) hydrate as phase change material for cooling lithium-ion battery in electric vehicle. J Power Sources 2019;427:70–6.
[122] Park S, Jang DS, Lee D, Hong SH, Kim Y. Simulation on cooling performance characteristics of a refrigerant-cooled active thermal management system for lithium ion batteries. Int J Heat Mass Tran 2019;135:131–41.
[123] An G, Xia X, Wu S, Liu Z, Wang L, Li S. Metal–organic frameworks for ammonia-based thermal energy storage. Small 2021;17:2102689.
[124] Xu J, Chao J, Li T, Yan T, Wu S, Wu M, et al. Near-zero-energy smart battery thermal management enabled by sorption energy harvesting from air. ACS Cent Sci 2020;6:1542–54.
[125] Deng Li, Xie Wu, Wang Yu, et al. Heat pipe thermal management based on high-rate discharge and pulse cycle tests for lithium-ion batteries. Energies 2019;12:3143.
[126] Elnaggar MHA, Abdullah MZ, Abdul Mujeebu M. Experimental analysis and FEM simulation of finned U-shape multi heat pipe for desktop PC cooling. Energy Convers Manag 2011;52:2937–44.
[127] Wang J-C. L-type heat pipes application in electronic cooling system. Int J Therm Sci 2011;50:97–105.
[128] Behi H, Behi M, Karimi D, Jaguemont J, Ghanbarpour M, Behnia M, et al. Heat pipe air-cooled thermal management system for lithium-ion batteries: high power applications. Appl Therm Eng 2021;183:116240.
[129] Mei N, Xu X, Li R. Heat Dissipation Analysis on the liquid cooling system coupled with a flat heat pipe of a lithium-ion battery. ACS Omega 2020;5:17431–41.
[130] Tran T-H, Harmand S, Desmet B, Filangi S. Experimental investigation on the feasibility of heat pipe cooling for HEV/EV lithium-ion battery. Appl Therm Eng 2014;63:551–8.
[131] Ye Y, Saw LH, Shi Y, Tay AAO. Numerical analyses on optimizing a heat pipe thermal management system for lithium-ion batteries during fast charging. Appl Therm Eng 2015;86:281–91.
[132] Ye Y, Shi Y, Saw LH, Tay AAO. Performance assessment and optimization of a heat pipe thermal management system for fast charging lithium ion battery packs. Int J Heat Mass Tran 2016;92:893–903.
[133] Zhao R, Gu J, Liu J. An experimental study of heat pipe thermal management system with wet cooling method for lithium ion batteries. J Power Sources 2015;273:1089–97.
[134] Wang Q, Jiang B, Xue QF, Sun HL, Li B, Zou HM, et al. Experimental investigation on EV battery cooling and heating by heat pipes. Appl Therm Eng 2015;88:54–60.
[135] Ye X, Zhao Y, Quan Z. Experimental study on heat dissipation for lithium-ion battery based on micro heat pipe array (MHPA). Appl Therm Eng 2018;130:74–82.
[136] Dan D, Yao C, Zhang Y, Zhang H, Zeng Z, Xu X. Dynamic thermal behavior of micro heat pipe array-air cooling battery thermal management system based on thermal network model. Appl Therm Eng 2019;162:114183.
[137] Ling Z, Wang F, Fang X, Gao X, Zhang Z. A hybrid thermal management system for lithium ion batteries combining phase change materials with forced-air cooling. Appl Energy 2015;148:403–9.
[138] Zhao J, Rao Z, Liu C, Li Y. Experimental investigation on thermal performance of phase change material coupled with closed-loop oscillating heat pipe (PCM/CLOHP) used in thermal management. Appl Therm Eng 2016;93:90–100.
[139] Wu W, Yang X, Zhang G, Chen K, Wang S. Experimental investigation on the thermal performance of heat pipe-assisted phase change material based battery thermal management system. Energy Convers Manag 2017;138:486–92.
[140] Jiang ZY, Qu ZG. Lithium–ion battery thermal management using heat pipe and phase change material during discharge–charge cycle: a comprehensive numerical study. Appl Energy 2019;242:378–92.
[141] Ling Z, Cao J, Zhang W, Zhang Z, Fang X, Gao X. Compact liquid cooling strategy with phase change materials for Li-ion batteries optimized using response surface methodology. Appl Energy 2018;228:777–88.
[142] Diao Y, Kang Y, Liang L, Zhao Y, Zhu T. Experimental investigation on the heat transfer performance of a latent thermal energy storage device based on flat miniature heat pipe arrays. Energy 2017;138:929–41.
[143] Wei Y, Agelin-Chaab M. Experimental investigation of a novel hybrid cooling method for lithium-ion batteries. Appl Therm Eng 2018;136:375–87.
[144] Naghavi MS, Ong KS, Badruddin IA, Mehrali M, Silakhori M, Metselaar HSC. Theoretical model of an evacuated tube heat pipe solar collector integrated with phase change material. Energy 2015;91:911–24.
[145] Gao X-L, Liu X-H, Xie W-L, Zhang L-S, Yang S-C. Multiscale observation of Li plating for lithium-ion batteries. Rare Met 2021;40:3038–48.
[146] Li Ht J, Wu P. Researches on heating low–temperature lithium–ion power battery in electric vehicles. IEEE

Please cite this article as: Jiang ZY et al., Recent progress in lithium-ion battery thermal management for a wide range of temperature and abuse conditions, International Journal of Hydrogen Energy, https://doi.org/10.1016/j.ijhydene.2022.01.008

Conference and Expo Transportation Electrification Asia–Pacific 2014:1–6.
[147] Pesaran Av A, Stuart T. Cooling and preheating of batteries in hybrid electric vehicles. 6th ASME–JSME Thermal Engineering Joint Conference; 2003. p. 1–7.
[148] Song Jbj HS, Lee BH, Shin DH, Kim BH, Kim TH. Experimental study on the effects of pre–heating a battery in a low–temperature environment. IEEE Vehicle Power and Propulsion Conference 2012:1198–201.
[149] Ji Y, Wang CY. Heating strategies for Li-ion batteries operated from subzero temperatures. Electrochim Acta 2013;107:664–74.
[150] Zhang SSXK, Jow TR. A new approach toward improved low temperature performance of Li-ion battery. Electrochem Commun 2002;11:928–32.
[151] Ling Z, Wen X, Zhang Z, Fang X, Gao X. Thermal management performance of phase change materials with different thermal conductivities for Li-ion battery packs operated at low temperatures. Energy 2018;144:977–83.
[152] Zhu J, Sun Z, Wei X, Dai H. An alternating current heating method for lithium-ion batteries from subzero temperatures. Int J Energy Res 2016;40:1869–83.
[153] Zhang J, Ge H, Li Z, Ding Z. Internal heating of lithium-ion batteries using alternating current based on the heat generation model in frequency domain. J Power Sources 2015;273:1030–7.
[154] Ruan H, Jiang J, Sun B, Zhang W, Gao W, Wang LY, et al. A rapid low-temperature internal heating strategy with optimal frequency based on constant polarization voltage for lithium-ion batteries. Appl Energy 2016;177:771–82.
[155] Zhu J, Sun Z, Wei X, Dai H, Gu W. Experimental investigations of an AC pulse heating method for vehicular high power lithium-ion batteries at subzero temperatures. J Power Sources 2017;367:145–57.
[156] Li J-q, Fang L, Shi W, Jin X. Layered thermal model with sinusoidal alternate current for cylindrical lithium-ion battery at low temperature. Energy 2018;148:247–57.
[157] Hao Ge JH, Zhang Jianbo, Li Zhe. Temperature-adaptive alternating current preheating of lithium-ion batteries with lithium deposition prevention. J Electrochem Soc 2016;163:A290–9.
[158] Wang CY, Zhang G, Ge S, Xu T, Ji Y, Yang XG, et al. Lithium-ion battery structure that self-heats at low temperatures. Nature 2016;529:515–8.
[159] Zhang G, Ge S, Xu T, Yang X-G, Tian H, Wang C-Y. Rapid self-heating and internal temperature sensing of lithium-ion batteries at low temperatures. Electrochim Acta 2016;218:149–55.
[160] Yang X-G, Zhang G, Wang C-Y. Computational design and refinement of self-heating lithium ion batteries. J Power Sources 2016;328:203–11.
[161] Yang X-G, Liu T, Wang C-Y. Innovative heating of large-size automotive Li-ion cells. J Power Sources 2017;342:598–604.
[162] Lei Z, Zhang Y, Lei X. Temperature uniformity of a heated lithium-ion battery cell in cold climate. Appl Therm Eng 2018;129:148–54.
[163] Lei Z, Zhang Y, Lei X. Improving temperature uniformity of a lithium-ion battery by intermittent heating method in cold climate. Int J Heat Mass Tran 2018;121:275–81.
[164] Qu ZG, Jiang ZY, Wang Q. Experimental study on pulse self–heating of lithium–ion battery at low temperature. Int J Heat Mass Tran 2019;135:696–705.
[165] Luo M, Song J, Ling Z, Zhang Z, Fang X. Phase change material coat for battery thermal management with integrated rapid heating and cooling functions from −40 °C to 50 °C. Mater Today Energy 2021;20:100652.
[166] Mohan S, Kim Y, Stefanopoulou AG. Energy-conscious warm-up of Li-ion cells from subzero temperatures. IEEE Trans Ind Electron 2016;63:2954–64.
[167] Zuniga M, Jaguemont J, Boulon L, Dube Y. Heating lithium-ion batteries with bidirectional current pulses. 2015 IEEE Vehicle Power and Propulsion Conference (VPPC). IEEE; 2015. p. 1–6.
[168] Soares R, Bessman A, Wallmark O, Lindbergh G, Svens P. An experimental setup with alternating current capability for evaluating large lithium-ion battery cells. Batteries 2018;4:38.
[169] Zhou C-C, Su Z, Gao X-L, Cao R, Yang S-C, Liu X-H. Ultra-high-energy lithium-ion batteries enabled by aligned structured thick electrode design. Rare Met 2021;41:14–20.
[170] Pang M-C, Yang K, Brugge R, Zhang T, Liu X, Pan F, et al. Interactions are important: linking multi-physics mechanisms to the performance and degradation of solid-state batteries. Mater Today 2021;49:145–83.
[171] Wang H, Shi W, Hu F, Wang Y, Hu X, Li H. Over-heating triggered thermal runaway behavior for lithium-ion battery with high nickel content in positive electrode. Energy 2021;224:120072.
[172] Wang Q, Mao B, Stoliarov SI, Sun J. A review of lithium ion battery failure mechanisms and fire prevention strategies. Prog Energy Combust Sci 2019;73:95–131.
[173] Gao Z, Zhang X, Xiao Y, Wang H, Li N. Influence of coupling of overcharge state and short-term cycle on the mechanical integrity behavior of 18650 Li-ion batteries subject to lateral compression. Int J Hydrogen Energy 2018;43:5261–71.
[174] Feng X, Sun J, Ouyang M, He X, Lu L, Han X, et al. Characterization of large format lithium ion battery exposed to extremely high temperature. J Power Sources 2014;272:457–67.
[175] Feng X, Sun J, Ouyang M, Wang F, He X, Lu L, et al. Characterization of penetration induced thermal runaway propagation process within a large format lithium ion battery module. J Power Sources 2015;275:261–73.
[176] Chen M, Dongxu O, Liu J, Wang J. Investigation on thermal and fire propagation behaviors of multiple lithium-ion batteries within the package. Appl Therm Eng 2019;157:113750.
[177] Hatchard TD, MacNeil DD, Basu A, Dahn JR. Thermal model of cylindrical and prismatic lithium-ion cells. J Electrochem Soc 2001;148:A755.
[178] Coman PT, Rayman S, White RE. A lumped model of venting during thermal runaway in a cylindrical Lithium Cobalt Oxide lithium-ion cell. J Power Sources 2016;307:56–62.
[179] Yeow KF, Teng H. Characterizing thermal runaway of lithium-ion cells in a battery system using finite element analysis approach. SAE Int J Alternative Powertrains 2013;2:179–86.
[180] Yang CKG, Sathanagopalan S, Pesaran A. Multi-physics modeling of thermal runaway propagation in a battery module. 2014. 223rd ECS Meeting.
[181] Feng X, Lu L, Ouyang M, Li J, He X. A 3D thermal runaway propagation model for a large format lithium ion battery module. Energy 2016;115:194–208.
[182] Spotnitz RM, Weaver J, Yeduvaka G, Doughty DH, Roth EP. Simulation of abuse tolerance of lithium-ion battery packs. J Power Sources 2007;163:1080–6.
[183] Smith K, Kim GH, Darcy E, Pesaran A. Thermal/electrical modeling for abuse-tolerant design of lithium ion modules. Int J Energy Res 2010;34:204–15.
[184] Feng X, He X, Ouyang M, Lu L, Peng W, Kulp C, et al. Thermal runaway propagation model for designing a safer battery pack with 25 Ah LiNi x Co y Mn z O 2 large format lithium ion battery. Appl Energy 2015;154:74–91.

Please cite this article as: Jiang ZY et al., Recent progress in lithium-ion battery thermal management for a wide range of temperature and abuse conditions, International Journal of Hydrogen Energy, https://doi.org/10.1016/j.ijhydene.2022.01.008

[185] Cho J. Dependence of AlPO4 coating thickness on overcharge behaviour of LiCoO2 cathode material at 1 and 2 C rates. J Power Sources 2004;126:186–9.
[186] Cho J, Kim H, Park B. Comparison of Overcharge Behavior of AlPO[sub 4]-Coated LiCoO[sub 2] and LiNi[sub 0.8]Co[sub 0.1]Mn[sub 0.1]O[sub 2] Cathode MaterialsinLi-IonCells. J Electrochem Soc 2004;151:A1707.
[187] Sun YK, Cho SW, Lee SW, Yoon CS, Amine K. AlF[sub 3]-coating to improve high voltage cycling performance of Li [Ni[sub 1/3]Co[sub 1/3]Mn[sub 1/3]]O[sub 2] cathode materials for lithium secondary batteries. J Electrochem Soc 2007;154:A168.
[188] Li G, Yang Z, Yang W. Effect of FePO4 coating on electrochemical and safety performance of LiCoO2 as cathode material for Li-ion batteries. J Power Sources 2008;183:741–8.
[189] Hu S-K, Cheng G-H, Cheng M-Y, Hwang B-J, Santhanam R. Cycle life improvement of ZrO2-coated spherical LiNi1/3Co1/3Mn1/3O2 cathode material for lithium ion batteries. J Power Sources 2009;188:564–9.
[190] Yun SH, Park K-S, Park YJ. The electrochemical property of ZrFx-coated Li[Ni1/3Co1/3Mn1/3]O2 cathode material. J Power Sources 2010;195:6108–15.
[191] Kobayashi H, Okumura T, Shikano M, Takada K, Arachi Y, Nitani H. The effects of Al2O3 coating on the performance of layered Li1.20Mn0.55Ni0.16Co0.09O2 materials for lithium-ion rechargeable battery. Solid State Ionics 2014;262:43–8.
[192] Cho W, Kim S-M, Song JH, Yim T, Woo S-G, Lee K-W, et al. Improved electrochemical and thermal properties of nickel rich LiNi 0.6 Co 0.2 Mn 0.2 O 2 cathode materials by SiO 2 coating. J Power Sources 2015;282:45–50.
[193] Cho W, Kim S-M, Lee K-W, Song JH, Jo YN, Yim T, et al. Investigation of new manganese orthophosphate Mn3(PO4) 2 coating for nickel-rich LiNi0.6Co0.2Mn0.2O2 cathode and improvement of its thermal properties. Electrochim Acta 2016;198:77–83.
[194] Ji W, Wang F, Liu D, Qian J, Cao Y, Chen Z, et al. Building thermally stable Li-ion batteries using a temperature-responsive cathode. J Mater Chem 2016;4:11239–46.
[195] Wilke S, Schweitzer B, Khateeb S, Al-Hallaj S. Preventing thermal runaway propagation in lithium ion battery packs using a phase change composite material: an experimental study. J Power Sources 2017;340:51–9.
[196] Xu J, Lan C, Qiao Y, Ma Y. Prevent thermal runaway of lithium-ion batteries with minichannel cooling. Appl Therm Eng 2017;110:883–90.
[197] Li Q, Yang C, Santhanagopalan S, Smith K, Lamb J, Steele LA, et al. Numerical investigation of thermal runaway mitigation through a passive thermal management system. J Power Sources 2019;429:80–8.
[198] Mohammadian SK, Zhang Y. Improving wettability and preventing Li-ion batteries from thermal runaway using microchannels. Int J Heat Mass Tran 2018;118:911–8.

Please cite this article as: Jiang ZY et al., Recent progress in lithium-ion battery thermal management for a wide range of temperature and abuse conditions, International Journal of Hydrogen Energy, https://doi.org/10.1016/j.ijhydene.2022.01.008